

## Article

# Porin-independent accumulation in *Pseudomonas* enables antibiotic discovery

<https://doi.org/10.1038/s41586-023-06760-8>

Received: 24 August 2022

Accepted: 18 October 2023

Published online: 22 November 2023

 Check for updates

Emily J. Geddes<sup>1</sup>, Morgan K. Gugger<sup>1</sup>, Alfredo Garcia<sup>1,3</sup>, Martin Garcia Chavez<sup>1,3</sup>, Myung Ryul Lee<sup>1</sup>, Sarah J. Perlmutter<sup>1</sup>, Christoph Bieniossek<sup>2</sup>, Laura Guasch<sup>2</sup> & Paul J. Hergenrother<sup>1,✉</sup>

Gram-negative antibiotic development has been hindered by a poor understanding of the types of compounds that can accumulate within these bacteria<sup>1,2</sup>. The presence of efflux pumps and substrate-specific outer-membrane porins in *Pseudomonas aeruginosa* renders this pathogen particularly challenging<sup>3</sup>. As a result, there are few antibiotic options for *P. aeruginosa* infections<sup>4</sup> and its many porins have made the prospect of discovering general accumulation guidelines seem unlikely<sup>5</sup>. Here we assess the whole-cell accumulation of 345 diverse compounds in *P. aeruginosa* and *Escherichia coli*. Although certain positively charged compounds permeate both bacterial species, *P. aeruginosa* is more restrictive compared to *E. coli*. Computational analysis identified distinct physicochemical properties of small molecules that specifically correlate with *P. aeruginosa* accumulation, such as formal charge, positive polar surface area and hydrogen bond donor surface area. Mode of uptake studies revealed that most small molecules permeate *P. aeruginosa* using a porin-independent pathway, thus enabling discovery of general *P. aeruginosa* accumulation trends with important implications for future antibiotic development. Retrospective antibiotic examples confirmed these trends and these discoveries were then applied to expand the spectrum of activity of a gram-positive-only antibiotic, fusidic acid, into a version that demonstrates a dramatic improvement in antibacterial activity against *P. aeruginosa*. We anticipate that these discoveries will facilitate the design and development of high-permeating antipseudomonals.

Antibiotic discovery for *Pseudomonas aeruginosa* has proven to be challenging, as achieving drug accumulation in these bacteria is particularly difficult compared to many other gram-negative pathogens<sup>3</sup>. This lower permeability of *P. aeruginosa* is in part because of the absence of non-specific porins, such as OmpF in *Escherichia coli*, which facilitate the diffusion of small, hydrophilic compounds across the outer membrane. Instead, *P. aeruginosa* possesses about 40 monomeric channels for nutrient transport with size restrictions of about 200 Da (ref. 6). Also, *P. aeruginosa* can express a broad range of tripartite efflux pumps, resulting in highly efficient antibiotic efflux<sup>7</sup>. This combination confers high intrinsic resistance to many antibiotics, including some that are commonly used to treat infections caused by other gram-negative pathogens; for example, although antibiotics such as chloramphenicol, tetracyclines and trimethoprim/sulfamethoxazole have clinical activity against other gram-negative organisms, they are not effective against *P. aeruginosa*<sup>4</sup>. The lack of clinical efficacy of these drugs is attributed to poor intracellular accumulation in *P. aeruginosa*, not to a lack of target engagement<sup>8</sup>. This is also true for antibiotics that are ‘gram-positive-only’ (for example, erythromycin, linezolid, fusidic acid (FA), rifampin and so on) and have no activity against any gram-negative pathogens<sup>8</sup>. Ultimately, only

four classes of antibiotics ( $\beta$ -lactams, fluoroquinolones, aminoglycosides and polymyxins) are used clinically to treat *P. aeruginosa* infections and with resistance rampant and significant toxicity of certain active classes (for example, aminoglycosides and polymyxins)<sup>9,10</sup>, new antibacterials for *P. aeruginosa* infections are an area of significant need.

The identification of physicochemical properties that promote intracellular compound accumulation would greatly aid in the development of new antipseudomonal antibiotics<sup>1,2,11,12</sup>. For example, an understanding of compound accumulation in *E. coli* has led to actionable guidelines<sup>11,13</sup> that have been used to imbue gram-negative antibacterial activity into many different classes of compounds<sup>14–25</sup>. However, despite important retrospective and prospective analyses of antibiotic activity and accumulation in *P. aeruginosa*<sup>8,26–28</sup>, general rules for compound accumulation in this bacterium have remained elusive. With many sources of potential uptake and efflux in *P. aeruginosa*, the possibility for discovery of generalizable accumulation guidelines for *P. aeruginosa* has been questioned<sup>5</sup>. Here, we use a whole-cell accumulation assay to assess the ability of non-antibiotic, structurally diverse small molecules to accumulate in this pathogen, ultimately leading to principles that will be helpful in the design of antipseudomonals.

<sup>1</sup>Department of Chemistry and Carl R. Woese Institute for Genomic Biology, University of Illinois, Urbana, IL, USA. <sup>2</sup>Roche Pharma Research and Early Development, Innovation Center Basel, F. Hoffmann-La Roche Ltd, Basel, Switzerland. <sup>3</sup>These authors contributed equally: Alfredo Garcia, Martin Garcia Chavez. <sup>✉</sup>e-mail: hergenro@illinois.edu

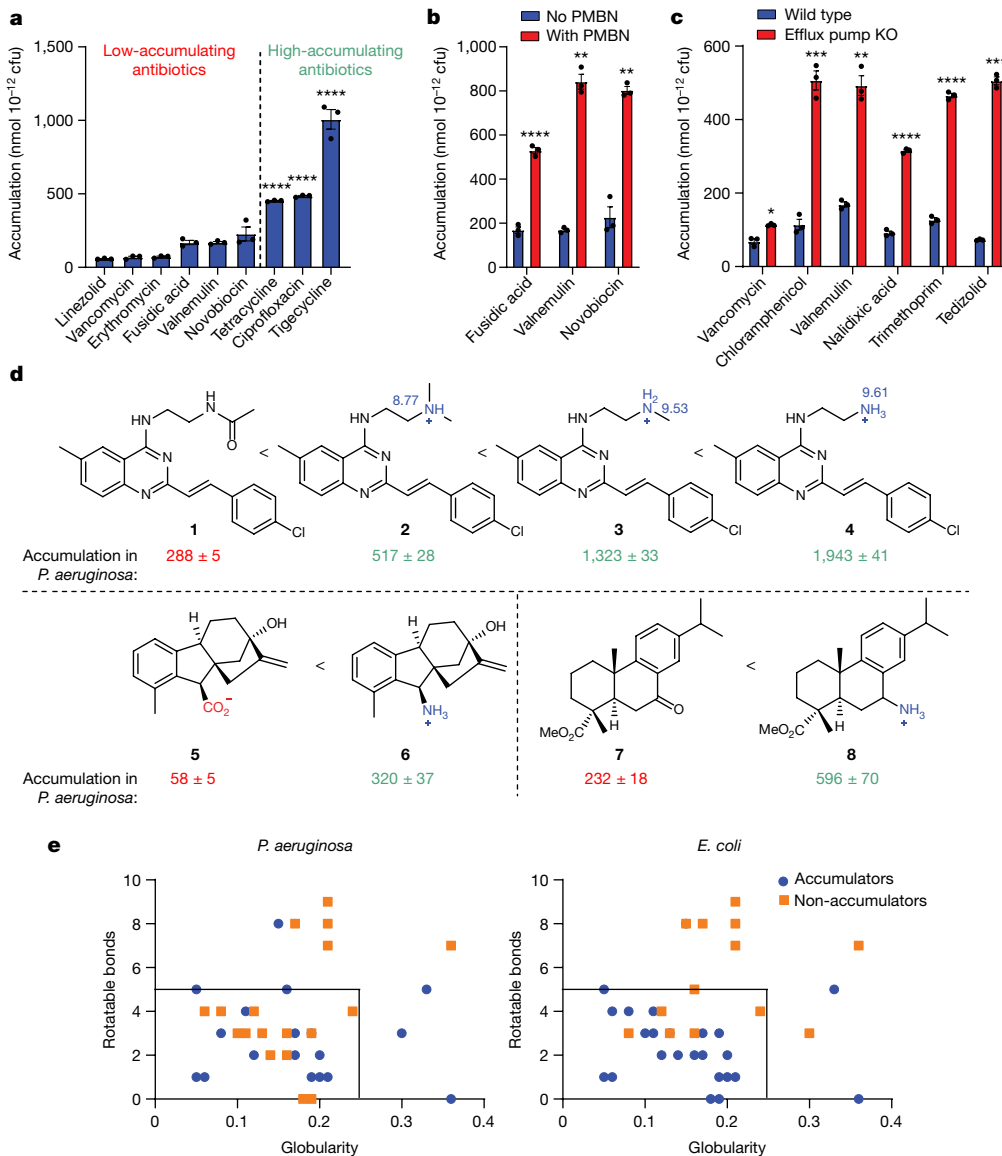


**Fig. 1 | Assessment of antibiotic controls in *P. aeruginosa* accumulation assay and evaluation of eNTRy rules predictability in *P. aeruginosa*.**

**a**, Inactive antibiotics show low accumulation in *P. aeruginosa* PAO1, whereas active antibiotics are high accumulators. Statistically significant accumulation above the average of the low-accumulating controls is indicated with asterisks: \*\*\* $P < 0.001$ ; tetracycline ( $P = 7.6 \times 10^{-5}$ ), ciprofloxacin ( $P = 3.1 \times 10^{-5}$ ), tigecycline ( $P = 1.6 \times 10^{-8}$ ). **b**, Low-accumulating antibiotics show an increase in accumulation with treatment of PMBN (8  $\mu\text{g ml}^{-1}$ ). Statistically significant accumulation differences for low-accumulating compounds in permeabilized and non-permeabilized PAO1 are indicated with asterisks: \*\* $P < 0.01$ , \*\*\* $P < 0.0001$ ; FA ( $P = 5.8 \times 10^{-5}$ ), valnemulin ( $P = 1.8 \times 10^{-3}$ ), novobiocin ( $P = 3.0 \times 10^{-3}$ ). **c**, Efflux substrates show increased accumulation in the efflux pump knockout (KO) strain, *P. aeruginosa* PAΔ6, whereas non-substrate vancomycin shows only minimal ( $P = 1.9 \times 10^{-2}$ ) increase. Statistically significant accumulation differences for low-accumulating compounds in wild-type *P. aeruginosa* PAO1 and efflux-deficient *P. aeruginosa* are indicated with asterisks: \* $P < 0.05$ , \*\* $P < 0.01$ , \*\*\* $P < 0.001$ ; chloramphenicol ( $P = 7.6 \times 10^{-4}$ ),

valnemulin ( $P = 4.5 \times 10^{-3}$ ), nalidixic acid ( $P = 9 \times 10^{-6}$ ), trimethoprim ( $P = 2 \times 10^{-6}$ ) and tedizolid ( $P = 5.3 \times 10^{-4}$ ). **d**, The influence of amines on accumulation in *P. aeruginosa* PAO1 for three different series of compounds. The  $\text{pK}_a$  values are shown in blue and were calculated using Chemaxon. For accumulation, green numbers indicate statistically significant accumulation values over the non-accumulating antibiotic controls, red numbers indicate non-statistically significant accumulation values over non-accumulating antibiotic controls. **e**, The influence of globularity and rotatable bonds on accumulation in *P. aeruginosa* PAO1 versus *E. coli* MG1655 for 40 primary amines. Low globularity and low rotatable bonds are predictive for about 80% of compounds tested in *E. coli* but only about 50% for *P. aeruginosa*. Structures of all compounds are in Supplementary Table 1 and the ‘Compound Master Table’ and data for *E. coli* are taken from ref. 13. For all figure panels, the average and s.e.m. are reported for accumulation values (nmol  $10^{-12}$  cfu).  $n = 3$  biologically independent samples. Statistical significance was determined using a two-sample Welch’s *t*-test (one-tailed test, assuming unequal variance).

## Validation of assay in *P. aeruginosa*

To study compound accumulation in *P. aeruginosa*, a liquid chromatography–mass spectrometry/mass spectrometry (LC–MS/MS)-based assay was used<sup>13,29</sup>. Although predominately used to examine compound accumulation in *E. coli*<sup>13–15,30</sup>, this assay has been used with *P. aeruginosa*<sup>15,28</sup>. To validate the assay, a selection of antibiotic controls were evaluated for

whole-cell accumulation in *P. aeruginosa* PAO1. This panel (Extended Data Table 1a) includes antibiotics with activity (minimum inhibitory concentration (MIC)  $\leq 16 \mu\text{g ml}^{-1}$ ) against *P. aeruginosa* in culture and antibiotics inactive against *P. aeruginosa* (MIC  $\geq 256 \mu\text{g ml}^{-1}$ ). The inactive antibiotics all showed minimal accumulation in PAO1, whereas the active antibiotics all demonstrated statistically significant amounts of accumulation relative to the inactive compounds (Fig. 1a). To further evaluate this assay

in *P. aeruginosa*, bacteria were treated with the membrane permeabilizer polymyxin B nonapeptide (PMBN)<sup>31</sup>. The low-accumulating antibiotics FA, valnemulin and novobiocin all showed a significant increase in accumulation upon membrane permeabilization, consistent with the assay not simply reporting on non-specific interactions with the outer membrane (Fig. 1b and Extended Data Table 1a). As an extra control, antibacterial activity and accumulation of low-accumulating antibiotics were also evaluated in a genetically modified strain of *P. aeruginosa* PAO1, which has six efflux pumps knocked out (PAΔ6)<sup>26</sup>. MIC ratios were used to identify efflux substrates (Extended Data Table 1b); an increase in accumulation in the PAΔ6 strain was observed for the antibiotics that were highly potentiated on efflux pump knockout (chloramphenicol, valnemulin, nalidixic acid, trimethoprim and tedizolid), although vancomycin, which shows no potentiation upon efflux pump knockout<sup>8</sup>, showed minimal change in accumulation in this experiment (Fig. 1c). Finally, to compare the results obtained by LC–MS/MS analysis to those obtained with fluorescence imaging, the accumulation of bisindolylmaleimide X (BIM X), an intrinsically fluorescent non-antibiotic, was evaluated in both *P. aeruginosa* PAO1 and *E. coli* MG1655. The LC–MS/MS assay revealed that BIM X accumulates in *P. aeruginosa* but not in *E. coli* (as described later) and confocal fluorescence imaging validated these results (Extended Data Fig. 1a,b).

## Comparison with eNTRy rules

To identify physicochemical properties that promote accumulation in *P. aeruginosa*, accumulation of a collection of diverse, non-antibiotic compounds was evaluated, including natural product-like compounds generated through the complexity-to-diversity strategy<sup>32</sup> and some commercially available compounds. As a main interest was defining how accumulation trends for *P. aeruginosa* compared to *E. coli*, a set of 67 compounds (Supplementary Table 1) whose accumulation was previously assessed in *E. coli*<sup>13</sup> was evaluated in *P. aeruginosa* PAO1.

In this set of 67 compounds, positive charge seemed to correlate with compound accumulation in *P. aeruginosa* PAO1, with all accumulating compounds being positively charged (Supplementary Table 1), as was observed for this same compound set in *E. coli* (Supplementary Table 1)<sup>13</sup>. The importance of positive charge for accumulation in *P. aeruginosa* was further demonstrated through side-by-side comparisons of similar compounds differing only in the nature of the charge. As shown with a series of 6-methylquinazolines, amine-containing versions accumulate in PAO1 much more than the corresponding neutral amide, with the primary amine leading to the highest amounts of accumulation among the set, probably because of both the increased steric accessibility and increased p*K*<sub>a</sub> (the negative log<sub>10</sub> of the dissociation constant of an acid) of the primary amine relative to the secondary and tertiary amine comparators (Fig. 1d; **1–4**). These data mirror trends seen in *E. coli* with the same compounds<sup>33</sup>. Other matched compound pairs (**5** and **6**, **7** and **8** in Fig. 1d) also demonstrate how a primary amine can facilitate compound accumulation in *P. aeruginosa* in certain contexts.

The importance of positive charge for compound accumulation, observed here for *P. aeruginosa*, invites comparison to the eNTRy rules (formulated for *E. coli*) which state that compounds with a positive charge (primary amine being best), low globularity and a low number of rotatable bonds are most likely to accumulate in *E. coli*<sup>11,13</sup>. To assess the applicability of the eNTRy rules to *P. aeruginosa*, data for the compounds bearing primary amines in the set of 67 compounds were plotted according to their number of rotatable bonds and globularity scores; for this analysis amines that did not meet the other criteria identified previously as important for accumulation (steric accessibility and low amphiphilic moment)<sup>13</sup> were removed, leaving a total of 40 compounds (see ‘Compound Master Table’ in the Supplementary Tables). This analysis revealed that low globularity and rotatable bonds were not predictive for accumulation in *P. aeruginosa*, as these cutoffs include many compounds that are non-accumulators in *P. aeruginosa*;

further, four compounds outside the eNTRy rules accumulate well in *P. aeruginosa*, with ultimately only around 50% of compounds binned correctly in this dataset (Fig. 1e). For *E. coli*, these cutoffs bin around 80% of all compounds correctly (Fig. 1e), consistent with previous results in *E. coli* for a large compound set<sup>13,33</sup>. These exceptions to the eNTRy rules in both directions suggest that, besides the beneficial introduction of a primary amine, the eNTRy rules do not predict compound accumulation in *P. aeruginosa*.

As not all compounds that possess a primary amine accumulate in *P. aeruginosa*, the compound test set was expanded to identify other properties that facilitate accumulation. In all, 240 primary amines (Supplementary Table 2) and 105 other compounds with varying charge states (Supplementary Table 3) were evaluated for accumulation in *P. aeruginosa* PAO1. Data gathered with this collection of 345 compounds confirmed the findings from the smaller compound set. It was observed that many positively charged compounds accumulate (Fig. 2a) and accumulators span a broad range of log of calculated distribution coefficient, octanol/buffer pH 7.4 (ClogD<sub>7.4</sub>) values (Fig. 2a). To make explicit head-to-head comparisons, accumulation of a large set of primary amines was assessed in both *P. aeruginosa* and *E. coli*. Analysis of these results for 154 compounds shows that, whereas around 80% of compounds meeting the eNTRy rule cutoffs accumulate in *E. coli*, in agreement with the original report<sup>13</sup>, the number of rotatable bonds and globularity are not useful for predicting accumulation in *P. aeruginosa*, with only around 40% of the compounds being sorted correctly as accumulators or non-accumulators in *P. aeruginosa* by the eNTRy rules (Extended Data Fig. 2a). Extended Data Fig. 2 also shows examples of compounds that accumulate in *E. coli* but not in *P. aeruginosa* (Extended Data Fig. 2b) and vice versa (for example, BIM X; Extended Data Fig. 2c).

Beyond the three eNTRy rule parameters, two other properties were previously identified as important for accumulation in *E. coli*, amphiphilic moment and amine steric accessibility<sup>13</sup>. Consistent with the observation in *E. coli*, increasing amphiphilic moment correlated with an increase in compound accumulation in *P. aeruginosa* (Extended Data Fig. 3a). The steric accessibility of amines also made a significant difference in accumulation values. As in *E. coli*, compounds with primary amines accumulated to a greater extent in *P. aeruginosa* than those with a secondary amine (Extended Data Fig. 3b). Also, compounds with primary amines on secondary carbons accumulated to a greater extent than compounds with primary amines on tertiary carbons (Extended Data Fig. 3c).

## Features influencing accumulation in *P. aeruginosa*

Although the presence of a sterically unencumbered primary amine on a compound with a high amphiphilic moment correlates with accumulation in *P. aeruginosa*, these traits are not enough to form a useful set of guidelines. Thus, we investigated other physicochemical traits that might facilitate accumulation in *P. aeruginosa*. For this work, a cheminformatic approach was used, starting with the calculation of 288 physicochemical properties for each of the 240 primary amines from Fig. 2a. These descriptors were used to train a random forest classification model to predict compound accumulation (Extended Data Fig. 4)<sup>13</sup>. Through this analysis, it was noted that hydrogen bond donor (HBD) surface area and positive charge descriptors were positively correlated with accumulation.

The most predictive descriptors associated with positive charge were positive polar surface area and formal charge. Although these two positive charge descriptors have commonalities, using both accounts for compounds that (1) may have a primary amine with a lower p*K*<sub>a</sub> and less localized charge but have other partially charged functional groups that are beneficial for accumulation (low formal charge, high positive polar surface area) and (2) are smaller compounds that may be highly charged but have lower overall surface area (high formal

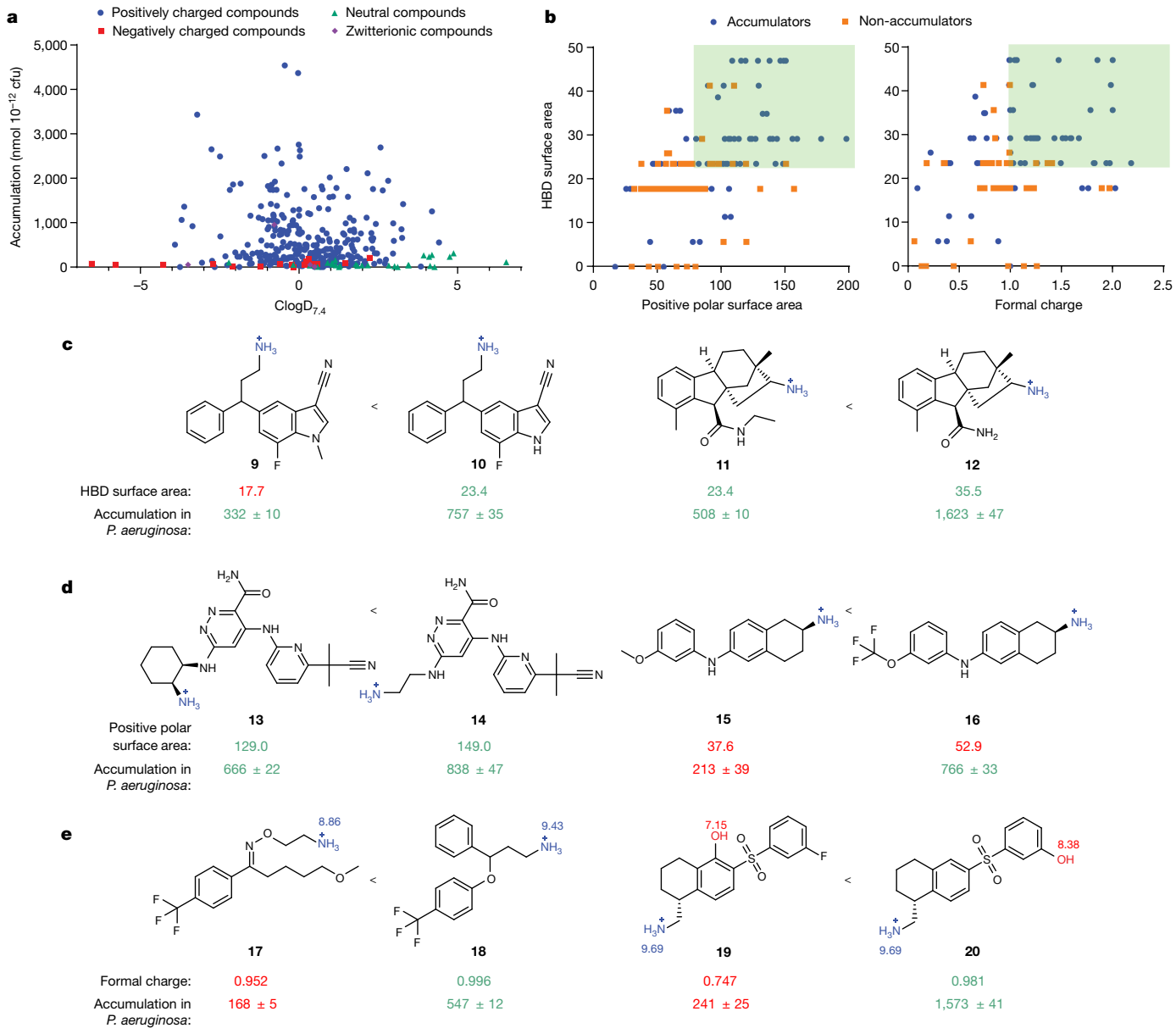


**Fig. 2 | Importance of ClogD<sub>7.4</sub>, HBD surface area and positive charge descriptors for accumulation in *P. aeruginosa* PAO1.** **a**, A set of 345 compounds, including 240 primary amines, was evaluated for accumulation in *P. aeruginosa* PAO1. All accumulating compounds have a positive charge. Structures, properties and accumulation are reported in Supplementary Tables 2 and 3 and include all 67 compounds from Supplementary Table 1. **b**, Analysis of 240 primary amines, correlation of formal charge or positive polar surface area and HBD surface area with compound accumulation in *P. aeruginosa* PAO1. In this analysis, compounds with HBD surface area  $\geq 23$  and either positive polar surface area  $\geq 80$  or formal charge  $\geq 0.98$  were most likely to accumulate. More than 80% of compounds that met these criteria were accumulators, shown in the green box. A total of 113 compounds met the criteria and 92 of them were accumulators, whereas 21 were non-accumulators. A total of 127 compounds did not meet the criteria and 55 of them were accumulators and 72 were non-accumulators. **c**, Increasing HBD surface area leads to an increase in accumulation in *P. aeruginosa* PAO1. For HBD surface area, green numbers indicate values within the HBD surface area cut off, red indicates values outside of this cut off. For accumulation, green numbers indicate statistically significant accumulation values over the non-accumulating antibiotic controls, red numbers indicate non-statistically significant accumulation values over non-accumulating antibiotic controls. **d**, Increasing the positive polar surface area positively

correlates with accumulation in *P. aeruginosa* PAO1. For positive polar surface area, green numbers indicate values within the positive polar surface area cut off, red indicates values outside of this cut off. For accumulation, green numbers indicate statistically significant accumulation values over the non-accumulating antibiotic controls, red numbers indicate non-statistically significant accumulation values over non-accumulating antibiotic controls. **e**, Increasing the formal charge of a molecule through pK<sub>a</sub> modulation of amines or other ionizable atoms increases accumulation in *P. aeruginosa* PAO1. Calculated pK<sub>a</sub> values for basic functionalities are shown in blue and calculated pK<sub>a</sub> values for acidic functionalities are shown in red. For formal charge, green numbers indicate values within the formal charge cut off, red indicates values outside of this cut off. For accumulation, green numbers indicate statistically significant accumulation values over the non-accumulating antibiotic controls, red numbers indicate non-statistically significant accumulation values over non-accumulating antibiotic controls. Accumulation units are reported in nmol  $10^{-12}$  cfu.  $n = 3$  biologically independent samples. The average and s.e.m. are reported for accumulation values. ClogD<sub>7.4</sub> was calculated using the online compound property calculation software FAFdrugs. Formal charge, HBD surface area (vs<sub>a</sub>\_don in MOE) and positive polar surface area (Q\_vs<sub>a</sub>\_PPos in MOE) were calculated in MOE. pK<sub>a</sub> values were calculated using Chemaxon.

charge, low positive polar surface area). Compounds with HBD surface area greater than or equal to 23 and with high positive charge (polar positive surface area greater than or equal to 80 and/or formal charge greater than or equal to 0.98) were most likely to accumulate (green boxes in Fig. 2b), with more than 80% (92 of 113) of all compounds that meet these criteria accumulating in *P. aeruginosa* PAO1. Side-by-side comparisons demonstrate the benefit of increasing HBD surface area (Fig. 2c; **9–12**), positive polar surface area (Fig. 2d; **13–16**) and formal charge, either through modulation of amine p*K<sub>a</sub>* (Fig. 2e; **17** and **18**) or through modulation of the p*K<sub>a</sub>* of other ionizable atoms (Fig. 2e; **19** and **20**). Further analysis of matched molecular pairs demonstrates a clear correlation between increased amine p*K<sub>a</sub>* (and increased amine steric accessibility) and higher compound accumulation in *P. aeruginosa* (Extended Data Fig. 3d and Supplementary Table 8). It is notable that overall accumulation values in *P. aeruginosa* PAO1 are still about 50% lower on average compared to *E. coli* MG1655, consistent with the increased permeability barrier of *P. aeruginosa* relative to other gram-negative pathogens (Extended Data Fig. 3e)<sup>34</sup>.

## Mode of uptake

With the importance of positive charge for accumulation in *P. aeruginosa* established and with a wide range of potential porins responsible for compound uptake in this organism, it was of interest to investigate the mode of uptake for these compounds. In an attempt to identify compounds that rely on substrate-specific channels of *P. aeruginosa* for uptake, accumulation was assessed for a subset of compounds in a strain of *P. aeruginosa* that has 40 putative porins knocked out (PA14 Δ40)<sup>35</sup> and accumulation values were compared to the parental strain, PA14. Compounds ranged in molecular weight from less than 200 Da to greater than 500 Da and included monoamines, diamines and guanidiniums (Supplementary Table 4). Most compounds showed no statistically significant difference in accumulation between the two strains, indicating that even the absence of 40 porins does not significantly alter accumulation (Fig. 3a). Only one compound (**31**) showed a statistically significant decrease in accumulation in the PA14 Δ40 strain, whereas four compounds (**22**, **29**, **35** and **46**) had slightly higher accumulation values. Suspecting the self-promoted uptake pathway<sup>36</sup> as the mode of permeation, the same subset of compounds was evaluated for accumulation in *P. aeruginosa* in media supplemented with MgCl<sub>2</sub>. Magnesium ions compete for lipopolysaccharide binding sites with cationic species and cotreatment is often used to identify compounds that use the self-promoted uptake pathway<sup>37</sup>. Notably, in *P. aeruginosa*, monoamines, diamines and guanidiniums showed substantially diminished accumulation in the presence of magnesium ions (Fig. 3b and see Extended Data Fig. 5a for confocal images of BIM X in the presence and absence of MgCl<sub>2</sub>), suggesting a significant role for the self-promoted uptake pathway for these compounds. The same experiment was performed in *E. coli* MG1655, in which both porin-mediated and self-promoted uptake are likely to be operative<sup>37</sup>. Although co-incubation with MgCl<sub>2</sub> did lower accumulation amounts in *E. coli* as expected, it was to a lesser extent than was observed for *P. aeruginosa* (Extended Data Fig. 5b). As a control, magnesium binding to a polycation (norspermine) was evaluated by nuclear magnetic resonance (NMR), revealing no/low binding, suggesting that it is unlikely that magnesium is simply reducing compound availability (Extended Data Fig. 5c). Accumulation in *P. aeruginosa* PAO1 was also evaluated in media supplemented with PMBN to weaken the lipopolysaccharide layer. Most compounds showed a statistically significant increase in accumulation, further supporting entry through the self-promoted uptake pathway (Extended Data Fig. 5d). These accumulation results indicate that, in contrast to other gram-negative species, *P. aeruginosa* does not primarily rely on porins for most small-molecule uptake; instead, self-promoted uptake probably accounts for most permeation into the cell.

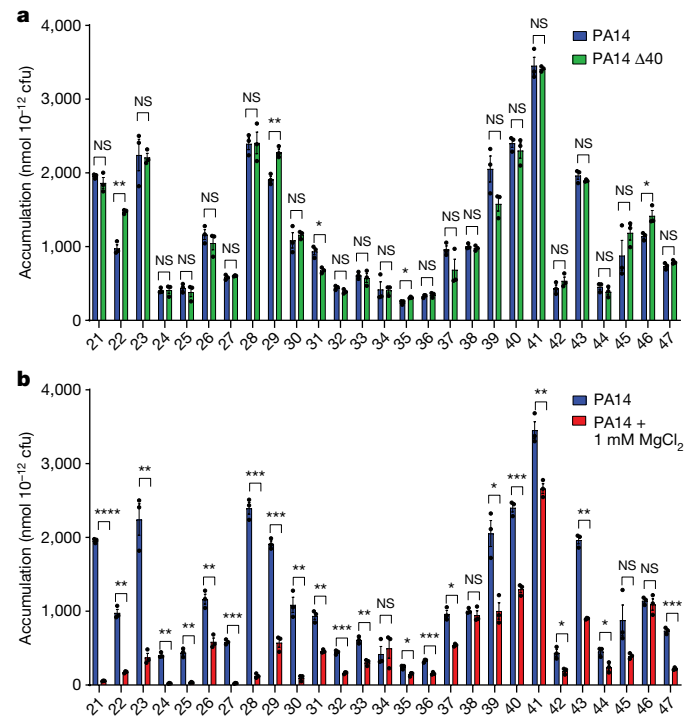


**Fig. 3 | Evaluation of accumulation in a porin-deficient strain and in the presence of magnesium.** **a**, Compounds tested in *P. aeruginosa* PA14 with all 40 putative porins knocked out (PA14 Δ40) show minimal accumulation differences relative to the parental strain PA14, suggesting a porin-independent mode of uptake. **b**, The same set of compounds shows a significant decrease in accumulation on cotreatment with MgCl<sub>2</sub> (1 mM), suggesting self-promoted uptake as the primary mode of entry for these compounds. The same PA14 data are used in Fig. 3a,b. All structures and accumulation values are listed in Supplementary Table 4a. *n* = 3 biologically independent samples. The average and s.e.m. are reported for accumulation values. Statistical significance was determined using a two-sample Welch's *t*-test (one-tailed test, assuming unequal variance). Statistically significant accumulation differences for compounds in *P. aeruginosa* PA14 versus *P. aeruginosa* PA14 with MgCl<sub>2</sub> treatment or *P. aeruginosa* PA14 Δ40 are indicated with asterisks (NS, not significant, \**P* < 0.05, \*\**P* < 0.01, \*\*\**P* < 0.001, \*\*\*\**P* < 0.0001).

## Accumulation of diamines

The importance of self-promoted uptake and positive charge for accumulation led us to examine the impact of many positive charges on accumulation. In two examples, it was observed that diamines exhibited higher accumulation values relative to their monoamine comparators (Extended Data Fig. 6a; **65–68**). Whereas diamines containing two primary amines are almost always high accumulators (Extended Data Fig. 6a,b), diamines with one primary amine and one secondary or tertiary amine less reliably provide an accumulation benefit in *P. aeruginosa* (Extended Data Fig. 6c).

## Accumulation of guanidiniums and pyridiniums

Guanidiniums and pyridiniums provide positively charged alternatives that are more lipophilic relative to primary amines and have previously been demonstrated to improve accumulation in *E. coli* to differing extents<sup>33</sup>. To assess the accumulation benefit of these functional groups in *P. aeruginosa*, a set of 16 amine, guanidinium and pyridinium side-by-side comparisons (48 compounds total) were evaluated for accumulation in *P. aeruginosa* PAO1. Guanidiniums had comparable accumulation values and classification relative to their primary amine comparators, whereas most pyridiniums led to a substantial

decrease in accumulation and were not classified as accumulators (Extended Data Fig. 6d,e and Supplementary Table 5); this result matches observations in *E. coli*<sup>33</sup>.

### Accumulation trends across *P. aeruginosa* strains

*P. aeruginosa* has a large pan-genome, leading to significant heterogeneity between strains<sup>38</sup>. To test the generality of the accumulation trends observed in *P. aeruginosa* PAO1, further representative strains of *P. aeruginosa* were selected. *P. aeruginosa* PA14 is a highly virulent strain that is a part of the most common clonal group and contains pathogenicity islands in its genome that are absent in PAO1 (ref. 39). Also, a clinical isolate from an acute infection, *P. aeruginosa* PA1280, was evaluated<sup>40</sup>. MICs for antibiotics against each of these strains were determined and intracellular accumulation was measured. Accumulation of these antibiotic controls correlated well with the observed activity (Extended Data Fig. 6f and Extended Data Table 1c).

More compounds were selected for evaluation of accumulation in PA14 and PA1280, comprising 27 non-antibiotics with a range of accumulation amounts in PAO1. Although some variance in overall values occurred and accumulation was on average lower in PA1280, very few compounds changed classification from ‘accumulator’ to ‘non-accumulator’ or vice versa in either strain, suggesting that the accumulation model will be robust across different *P. aeruginosa* strains (Extended Data Fig. 6g and full dataset reported in Supplementary Table 6).

### Retrospective examples

A retrospective analysis of the literature was performed to assess whether previous serendipitous incorporation of these physicochemical properties had proved beneficial in historical drug discovery campaigns. Six examples of antibiotic pairs were identified in which one derivative had low whole-cell activity against *P. aeruginosa* but another derivative was reported with improved activity. These antibiotics are from diverse structural classes and engage a variety of biological targets, including DNA gyrase and topoisomerase (17x and 17r (ref. 16); AMQ-1 and AMQ-2 (ref. 19); THP-1 and THP-2 (ref. 41)), the ribosome (CHD and CDCHD<sup>18</sup>; tetracycline and tigecycline<sup>42</sup>) and the bacterial type 1 signal peptidase (G8126 and G0775, all structures in Extended Data Table 2)<sup>43</sup>. As biochemical potency and accumulation both contribute to whole-cell activity, where possible we aimed to select side-by-side comparisons of compounds with similar target engagement. MIC values in efflux pump-deficient strains were used as a surrogate for target engagement (Extended Data Table 2) and many of the reported pairs demonstrated similar activity in efflux pump-deficient bacterial strains. The HBD surface area and formal charge/positive polar surface area were calculated for these antibiotic pairs. Increasing HBD surface area to more than or equal to 23 and positive polar surface area to more than or equal to 80 led to an increase in antibacterial activity against *P. aeruginosa*, ranging from 4- to more than 32-fold improvements (data plotted in Fig. 4; structures and activity reported in Extended Data Table 2)<sup>16,18,19,41,43</sup>, suggesting that increased accumulation is a significant contributor to the observed improvement in antibacterial activity. Indeed, as shown in Fig. 1a, we find tigecycline accumulates to a higher extent than tetracycline. Further, when considering antibiotics used for the treatment of *P. aeruginosa* infections, both classes of positively charged antibiotics (aminoglycosides and polymyxins) match these guidelines for *P. aeruginosa* accumulation. These results indicate these guidelines as a generalizable means to increase accumulation in *P. aeruginosa* across a variety of scaffolds and targets.  $\beta$ -lactam and fluoroquinolone antibiotics meet the guidelines less consistently, probably due to their zwitterionic or negatively charged states.

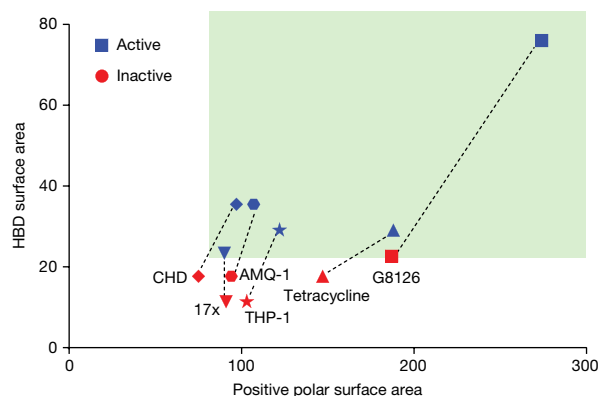


**Fig. 4 | Six retrospective examples in which an antibiotic derivative is more active (more than fourfold) against *P. aeruginosa* than the parent.** Analysis shows that the derivatives with improved antibacterial activity meet the HBD surface area and charge requirements for accumulation in *P. aeruginosa* (as shown by the green box). Target engagement (inferred from MIC values against efflux-deficient strains) is similar for most of the compound pairs (for structures of each antibiotic, see Extended Data Table 2), suggesting that the improved antibiotic activity against *P. aeruginosa* is due to an increase in accumulation; this has been explicitly shown as tetracycline/tigecycline pair (Fig. 1a).

### *P. aeruginosa*-active FA derivative

With an improved understanding of the physicochemical properties that promote intracellular accumulation, as well as the porin-independent mode of uptake of these compounds, we were interested in applying these findings to develop an antipseudomonal. Our discoveries suggest that increasing the HBD surface area and the formal charge and/or positive polar surface area of an antibiotic candidate should lead to improved whole-cell antibacterial activity against *P. aeruginosa* if target binding is not disrupted. As stated previously, there are many antibiotics (Extended Data Table 1d) that would have activity against *P. aeruginosa* if they could achieve higher intracellular accumulation. FA, a potent gram-positive-only antibiotic, is one example. FA has negligible whole-cell antibacterial activity in *P. aeruginosa* ( $\text{MIC} = 1,024 \mu\text{g ml}^{-1}$  versus PAO1; Fig. 5a) and poor intracellular accumulation (Fig. 5b). Notably, FA has an  $\text{MIC}$  of  $4 \mu\text{g ml}^{-1}$  against *P. aeruginosa* PAO1 when co-administering PMBN (Fig. 5a), as well as elevated accumulation in the presence of PMBN (Fig. 5b), suggesting that its biological target (elongation factor G, EF-G<sup>44</sup>) can be engaged in *P. aeruginosa* and that if FA could achieve higher intracellular concentrations, it would have whole-cell antibacterial activity.

With an HBD surface area of 0 and a positive polar surface area of 65.3 (Fig. 5c), FA does not meet our guidelines for accumulation in *P. aeruginosa* and was selected as a challenging starting point for conversion to a version active against this pathogen. Using the established structure–activity relationship of FA along with the accumulation guidelines for *P. aeruginosa*, FA derivatives were designed and synthesized. As the carboxylic acid is a convenient handle for structural modifications but necessary for target engagement<sup>45</sup>, we envisioned using a prodrug approach to increase permeation into the cell, while maintaining on-target activity against EF-G through the release of free FA inside the cell. An amidoxime prodrug moiety was ultimately selected as it was hydrolytically cleaved within a biologically relevant timeframe, liberating FA (Extended Data Fig. 8a). Amidoxime prodrug derivatives containing functional groups whose presence increases overall HBD surface area and positive polar surface area were synthesized and evaluated. Data collected in both *P. aeruginosa* PAO1 and *E. coli* MG1655 demonstrate a substantial increase in accumulation for all FA prodrug derivatives tested (Extended Data Fig. 7a). Accumulation

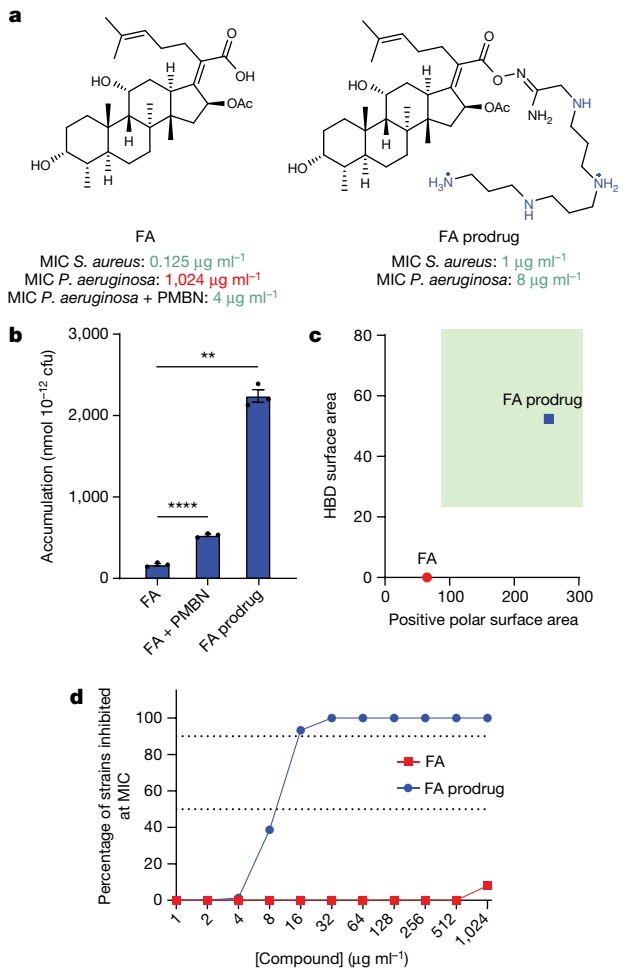


**Fig. 5 | Development of PA-active FA derivative.** **a**, FA has potent activity against gram-positive bacteria but no activity against *P. aeruginosa* PAO1. However, when co-administering the membrane permeabilizer PMBN ( $8 \mu\text{g ml}^{-1}$ ), FA has good antibacterial activity, indicating that the target (EF-G) can be exploited and if FA could accumulate, it would be active against wild-type *P. aeruginosa*. To improve accumulation using the predictive guidelines for *P. aeruginosa*, although maintaining the necessary acid for FA activity, an amidoxime prodrug moiety was generated with a polyamine linker. The prodrug is cleaved through hydrolysis to release FA inside the cell, leading to an MIC value of  $8 \mu\text{g ml}^{-1}$ , a 128-fold improvement in activity against wild-type *P. aeruginosa*. Green indicates active as antibiotic, and red indicates inactive antibiotic. **b**, FA accumulation in *P. aeruginosa* PAO1 is enhanced in the presence of PMBN ( $8 \mu\text{g ml}^{-1}$ ). FA prodrug shows more than 20 times higher accumulation compared with FA. As the prodrug hydrolyses under assay conditions, the accumulation of FA is reported for FA prodrug. **c**, FA does not meet the predictive guidelines for accumulation in *P. aeruginosa*, whereas FA prodrug fits the described physicochemical properties, highlighted in the green box. **d**, FA prodrug possesses  $64\text{--}256\times$  improved activity relative to FA against a panel of 75 clinical isolates of *P. aeruginosa*. MICs were performed in LB Lennox broth according to the CLSI guidelines in biological triplicate. Accumulation units are reported in  $\text{nmol } 10^{-12} \text{ cfu}$ .  $n = 3$  biologically independent samples. The average and s.e.m. are reported for accumulation values. Statistical significance was determined using a two-sample Welch's *t*-test (one-tailed test, assuming unequal variance). Statistically significant accumulation differences for FA in the presence of PBMN or with the prodrug linker are indicated with asterisks (\*\* $P < 0.01$ , \*\*\* $P < 0.0001$ ).

values increase with the number of amines, with the version containing four ionizable nitrogens (FA prodrug, Fig. 5a) demonstrating the highest accumulation (Extended Data Fig. 7a). FA prodrug meets the HBD surface area and positive polar surface area requirements for

accumulation in *P. aeruginosa* (Fig. 5c) and does indeed achieve very high accumulation amounts in PAO1 (Fig. 5b; accumulation reported for free FA). FA prodrug has an MIC of  $8 \mu\text{g ml}^{-1}$  against *P. aeruginosa* PAO1, a 128-fold increase relative to FA (Fig. 5a) and has MIC values of  $8\text{--}16 \mu\text{g ml}^{-1}$  against a panel of 75 clinical isolates of *P. aeruginosa*; FA has essentially no antibacterial activity against this clinical isolate panel (Fig. 5d and MIC values in Supplementary Table 7).

To explore the antibacterial mode of action of FA prodrug, *E. coli* MG1655 mutants resistant to FA prodrug were generated using a serial exposure method. Mutants that were viable at  $2\times$ ,  $4\times$  and  $8\times$  the MIC concentration were isolated. Resistant colonies showed a 4–8-fold increase in MIC values against FA prodrug and mutations map back to the FA binding pocket in EF-G indicating that liberated FA can engage its intracellular target and exert antibacterial activity (Extended Data Fig. 7b). Generation of *P. aeruginosa* PAO1 mutants resistant to FA prodrug was achieved using the large inoculum method, with a frequency of resistance at  $2.67 \times 10^{-7}$ . When sequenced, these mutants did not have mutations in *fusA*, indicating that FA prodrug probably has more than one mechanism of action.

The mode of action of FA prodrug in *P. aeruginosa* was then probed using structural derivatives. It is known that diacylation of FA significantly reduces antibacterial activity and indeed this compound (FA  $\text{Ac}_2\text{O}$ ) has an MIC =  $64 \mu\text{g ml}^{-1}$  in *Staphylococcus aureus* (Extended Data Fig. 7c). To evaluate the dependence of FA prodrug activity on inhibition of EF-G, a diacetylated version, FA prodrug  $\text{Ac}_2\text{O}$ , was synthesized (Extended Data Fig. 7c). This compound loses antibacterial activity against *P. aeruginosa* relative to FA prodrug, suggesting that some antibacterial activity of FA prodrug is derived from the inhibition of EF-G, with prodrugs with more amines providing more antibacterial activity through membrane depolarization (Extended Data Fig. 7a).

It is apparent that FA prodrug has a dual mode of antibacterial activity. On the basis of the polyamine moiety, we hypothesized that membrane-based interactions may be contributing to the antibacterial activity and a variety of experiments were performed to characterize such interactions. Cotreatment with  $\text{MgCl}_2$  led to a 32-fold shift in MIC for FA prodrug and gentamicin in *P. aeruginosa* PAO1, whereas FA showed no change in antibacterial activity, suggesting that FA prodrug entry into *P. aeruginosa* occurs through the self-promoted uptake pathway (Extended Data Fig. 8b); NaCl had minimal effects in the same experiment (Extended Data Fig. 8b). The fluorescent probe *N*-phenylnaphthalimide (NPN) was used to assess outer-membrane permeability changes on treatment with FA, gentamicin, colistin and FA prodrug. NPN is membrane impermeable and is only weakly fluorescent in aqueous solutions. On entry to the cell and interacting with phospholipids, significant fluorescence is observed. Whereas treatment of *P. aeruginosa* PAO1 with FA for 10 minutes did not lead to any change in fluorescence, treatment with gentamicin, colistin and FA prodrug led to a dose-dependent increase (Extended Data Fig. 8c). Finally, using the potentiometric dye DiSC<sub>3</sub> (5), it was demonstrated that treatment with FA prodrug leads to dose-dependent inner-membrane depolarization, monitored by an increase in fluorescence, whereas treatment with FA did not affect membrane polarization (Extended Data Fig. 8d). All these data are consistent with FA prodrug relying on membrane interactions to enter the cell; in addition to the liberated FA engaging EF-G to kill the bacterial cells, inner-membrane depolarization by FA prodrug probably plays a role in the observed antibacterial activity. This residual membrane depolarizing antibacterial activity can be observed in the diacylated compound (Extended Data Fig. 7c). This effect can also be observed amongst the different versions of the FA prodrug, in which potency is not solely impacted by high accumulation values, as extending the polyamine moiety increases membrane-disrupting ability in addition to increasing accumulation (Extended Data Fig. 7a).

## Discussion

Comparison of results from the unbiased accumulation experiments in *E. coli* and *P. aeruginosa* highlights the benefit of ionizable nitrogens (with minimal steric encumbrance) and high amphiphilic moment to promote intracellular accumulation in both *E. coli* and *P. aeruginosa*. HBD surface area and positive charge parameters were found to positively correlate with accumulation in *P. aeruginosa* and about 80% of compounds that meet the appropriate cutoffs accumulate. As evidenced by this study, the unbiased evaluation of diverse non-antibiotic compounds can identify properties that are not apparent in the assessment of antibiotics.

An interesting and surprising result is the observed porin-independent uptake of compounds in *P. aeruginosa*. Assessing compound accumulation in a strain of *P. aeruginosa* with 40 putative porins knocked out ( $\Delta 40$ ) demonstrates few significant accumulation differences in the absence of porins. Consistent with our result, a similar trend was observed in assessing MIC values for antibiotics in the wild-type and  $\Delta 40$  strain; aside from the carbapenem antibiotics, no antibiotics had an MIC fold change in this study<sup>35</sup>. Collectively, these results indicate that in contrast to *E. coli*, in which the general porin OmpF facilitates uptake for some monoamines<sup>13,46</sup>, in *P. aeruginosa* the self-promoted uptake pathway may be the primary mode of uptake for all positively charged compounds. Multicharged antibiotics, such as the aminoglycosides and colistin, have been suggested to use this pathway for uptake into bacteria but the use of this pathway for monoamine uptake had not yet been disclosed. Evidence does suggest the importance of porin-mediated uptake for some negatively charged compounds into *P. aeruginosa*, most recently demonstrated by the rational design of ETX0462, which was chemically optimized for uptake through *P. aeruginosa* porins<sup>47</sup>. The development of a prodrug moiety that can facilitate self-promoted uptake into *P. aeruginosa* for FA may prove generalizable for other antibiotics in which antibacterial activity is limited because of poor intracellular accumulation; of course, as polyamine functionality can introduce liabilities (toxicity or off-target membrane interactions), optimization and exploration of other prodrugs will be beneficial.

Historical data and trends from the literature begin to make more sense in light of the results presented herein. For example, the impenetrability of *P. aeruginosa*, even relative to other gram-negative bacteria, has been noted by others and is powerfully shown (in comparison to *E. coli*) in Extended Data Fig. 3e. As certain small molecules can enter *E. coli* through porins, the general impenetrability of *P. aeruginosa* seems to be linked to the squelching of most porin-dependent uptake pathways. The inability to exploit porin-mediated uptake in *P. aeruginosa* has stymied antibiotic development for this pathogen but data presented herein suggest that purposeful design of antibiotics to leverage porin-independent mechanisms can be fruitful in the generation of antibiotics for this dangerous pathogen.

## Online content

Any methods, additional references, Nature Portfolio reporting summaries, source data, extended data, supplementary information, acknowledgements, peer review information; details of author contributions and competing interests; and statements of data and code availability are available at <https://doi.org/10.1038/s41586-023-06760-8>.

- Silver, L. L. A Gestalt approach to Gram-negative entry. *Bioorg. Med. Chem.* **24**, 6379–6389 (2016).
- Payne, D. J., Gwynn, M. N., Holmes, D. J. & Pompiano, D. L. Drugs for bad bugs: confronting the challenges of antibacterial discovery. *Nat. Rev. Drug. Discov.* **6**, 29–40 (2007).
- Yoshimura, F. & Nikaido, H. Permeability of *Pseudomonas aeruginosa* outer membrane to hydrophilic solutes. *J. Bacteriol.* **152**, 636–642 (1982).
- Bassetti, M., Vena, A., Croatto, A., Righi, E. & Guery, B. How to manage *Pseudomonas aeruginosa* infections. *Drugs Context* **7**, 212527 (2018).
- Tomasini, R., Iyer, R. & Miller, A. A. Antibacterial drug discovery: some assembly required. *ACS Infect. Dis.* **4**, 686–695 (2018).
- Tamber, S., Ochs, M. M. & Hancock, R. E. Role of the novel OprD family of porins in nutrient uptake in *Pseudomonas aeruginosa*. *J. Bacteriol.* **188**, 45–54 (2006).
- Aeschlimann, J. R. The role of multidrug efflux pumps in the antibiotic resistance of *Pseudomonas aeruginosa* and other Gram-negative bacteria. Insights from the Society of Infectious Diseases Pharmacists. *Pharmacotherapy* **23**, 916–924 (2003).
- Krishnamoorthy, G. et al. Synergy between active efflux and outer membrane diffusion defines rules of antibiotic permeation into Gram-negative bacteria. *mBio* **8**, e01172–17 (2017).
- Falagas, M. E. & Kasiakou, S. K. Toxicity of polymyxins: a systematic review of the evidence from old and recent studies. *Crit. Care* **10**, R27 (2006).
- Mingeot-Leclercq, M. P. & Tulkens, P. M. Aminoglycosides: nephrotoxicity. *Antimicrob. Agents Chemother.* **43**, 1003–1012 (1999).
- Richter, M. F. & Hergenrother, P. J. The challenge of converting Gram-positive-only compounds into broad-spectrum antibiotics. *Ann. N. Y. Acad. Sci.* **1435**, 18–38 (2019).
- Zgurskaya, H. I. & Rybenkov, V. V. Permeability barriers of Gram-negative pathogens. *Ann. N. Y. Acad. Sci.* **1459**, 5–18 (2020).
- Richter, M. F. et al. Predictive compound accumulation rules yield a broad-spectrum antibiotic. *Nature* **545**, 299–304 (2017).
- Motika, S. E. et al. Antibiotic active through inhibition of an essential riboswitch. *J. Am. Chem. Soc.* **142**, 10856–10862 (2020).
- Parker, E. N. et al. Implementation of permeation rules leads to a FabI inhibitor with activity against Gram-negative pathogens. *Nat. Microbiol.* **5**, 67–75 (2020).
- Hu, Y. et al. Discovery of pyrido[2,3-b]indole derivatives with Gram-negative activity targeting both DNA gyrase and topoisomerase IV. *J. Med. Chem.* **63**, 9623–9649 (2020).
- Andrews, L. D. et al. Optimization and mechanistic characterization of pyridopyrimidine inhibitors of bacterial biotin carboxylase. *J. Med. Chem.* **62**, 7489–7505 (2019).
- Lukežić, T. et al. Engineering atypical tetracycline formation in *Amycolatopsis sulphurea* for the production of modified chelocardin antibiotics. *ACS Chem. Biol.* **14**, 468–477 (2019).
- Skepper, C. K. et al. Topoisomerase inhibitors addressing fluoroquinolone resistance in Gram-negative bacteria. *J. Med. Chem.* **63**, 7773–7816 (2020).
- Brem, J. et al. Imitation of beta-lactam binding enables broad-spectrum metallo-beta-lactamase inhibitors. *Nat. Chem.* **14**, 15–24 (2022).
- Schumacher, C. E. et al. Total synthesis and antibiotic properties of amino-functionalized aromatic terpenoids related to erogorgiaene and the pseudopterosins. *Eur. J. Org. Chem.* **2022**, e202200058 (2022).
- Parker, E. N. et al. An iterative approach guides discovery of the FabI inhibitor fabimycin, a late-stage antibiotic candidate with in vivo efficacy against drug-resistant Gram-negative infections. *ACS Cent. Sci.* **8**, 1145–1158 (2022).
- Huang, K.-J. et al. Deletion of a previously uncharacterized lipoprotein lrl confers resistance to an inhibitor of type II signal peptidase in *Acinetobacter baumannii*. *Proc. Natl. Acad. Sci. USA* **119**, e212311719 (2022).
- Onyedibe, K. I. et al. Re-sensitization of multidrug-resistant and colistin-resistant Gram-negative bacteria to colistin by Povarov/Doebner-derived compounds. *ACS Infect. Dis.* **9**, 283–295 (2023).
- Goethe, O., DiBello, M. & Herzon, S. B. Total synthesis of structurally diverse pleuromutilin antibiotics. *Nat. Chem.* **14**, 1270–1277 (2022).
- Cooper, C. J. et al. Molecular properties that define the activities of antibiotics in *Escherichia coli* and *Pseudomonas aeruginosa*. *ACS Infect. Dis.* **4**, 1223–1234 (2018).
- Mehla, J. et al. Predictive rules of efflux inhibition and avoidance in *Pseudomonas aeruginosa*. *mBio* **12**, e02785–20 (2021).
- Leus Inga, V. et al. Functional diversity of Gram-negative permeability barriers reflected in antibacterial activities and intracellular accumulation of antibiotics. *Antimicrob. Agents Chemother.* **67**, e01377–22 (2023).
- Geddes, E. J., Li, Z. & Hergenrother, P. J. An LC-MS/MS assay and complementary web-based tool to quantify and predict compound accumulation in *E. coli*. *Nat. Protoc.* **16**, 4833–4854 (2021).
- Wallace, M. J. et al. Discovery and characterization of the antimetabolite action of thioacetamide-linked 1,2,3-triazoles as disruptors of cysteine biosynthesis in Gram-negative bacteria. *ACS Infect. Dis.* **6**, 467–478 (2020).
- Vaara, M. Agents that increase the permeability of the outer membrane. *Microbiol. Rev.* **56**, 395–411 (1992).
- Huigen, R. W. 3rd et al. A ring-distortion strategy to construct stereochemically complex and structurally diverse compounds from natural products. *Nat. Chem.* **5**, 195–202 (2013).
- Perlmutter, S. J. et al. Compound uptake into *E. coli* can be facilitated by N-alkyl guanidiniums and pyridiniums. *ACS Infect. Dis.* **7**, 162–173 (2021).
- Hancock, R. E. & Woodruff, W. A. Roles of porin and beta-lactamase in beta-lactam resistance of *Pseudomonas aeruginosa*. *Rev. Infect. Dis.* **10**, 770–775 (1988).
- Ude, J. et al. Outer membrane permeability: antimicrobials and diverse nutrients bypass porins in *Pseudomonas aeruginosa*. *Proc. Natl. Acad. Sci. USA* **118**, e2107644118 (2021).
- Loh, B., Grant, C. & Hancock, R. E. Use of the fluorescent probe 1-N-phenylnaphthylamine to study the interactions of aminoglycoside antibiotics with the outer membrane of *Pseudomonas aeruginosa*. *Antimicrob. Agents Chemother.* **26**, 546–551 (1984).
- Hancock, R. E. & Farmer, S. W. Mechanism of uptake of deglucoteicoplanin amide derivatives across outer membranes of *Escherichia coli* and *Pseudomonas aeruginosa*. *Antimicrob. Agents Chemother.* **37**, 453–456 (1993).
- Kung, V. L., Ozer, E. A. & Hauser, A. R. The accessory genome of *Pseudomonas aeruginosa*. *Microbiol. Mol. Biol. Rev.* **74**, 621–641 (2010).
- Mikkelsen, H., McMullan, R. & Filloux, A. The *Pseudomonas aeruginosa* reference strain PA14 displays increased virulence due to a mutation in lads. *PLoS ONE* **6**, e29113 (2011).
- Williams, J. J., Halvorsen, E. M., Dwyer, E. M., DiFazio, R. M. & Hergenrother, P. J. Toxin-antitoxin (TA) systems are prevalent and transcribed in clinical isolates of *Pseudomonas*

- aeruginosa* and methicillin-resistant *Staphylococcus aureus*. *FEMS Microbiol. Lett.* **322**, 41–50 (2011).
41. Surivet, J. P. et al. Synthesis and characterization of tetrahydropyran-based bacterial topoisomerase inhibitors with antibacterial activity against Gram-negative bacteria. *J. Med. Chem.* **60**, 3776–3794 (2017).
42. Sum, P. E. et al. Glycylcyclines. 1. A new generation of potent antibacterial agents through modification of 9-aminotetradecyclines. *J. Med. Chem.* **37**, 184–188 (1994).
43. Smith, P. A. et al. Optimized arylomycins are a new class of Gram-negative antibiotics. *Nature* **561**, 189–194 (2018).
44. Tanaka, N., Kinoshita, T. & Masukawa, H. Mechanism of protein synthesis inhibition by FA and related antibiotics. *Biochem. Biophys. Res. Commun.* **30**, 278–283 (1968).
45. Garcia Chavez, M. et al. Synthesis of FA derivatives yields a potent antibiotic with an improved resistance profile. *ACS Infect. Dis.* **7**, 493–505 (2021).
46. Haloi, N. et al. Rationalizing the generation of broad spectrum antibiotics with the addition of a positive charge. *Chem. Sci.* **12**, 15028–15044 (2021).
47. Durand-Reville, T. F. et al. Rational design of a new antibiotic class for drug-resistant infections. *Nature* **597**, 698–702 (2021).

**Publisher's note** Springer Nature remains neutral with regard to jurisdictional claims in published maps and institutional affiliations.

Springer Nature or its licensor (e.g. a society or other partner) holds exclusive rights to this article under a publishing agreement with the author(s) or other rightsholder(s); author self-archiving of the accepted manuscript version of this article is solely governed by the terms of such publishing agreement and applicable law.

© The Author(s), under exclusive licence to Springer Nature Limited 2023

## Methods

### Bacterial strains

*P. aeruginosa* PAO1 and *E. coli* MG1655 were obtained from the American Type Culture Collection. *P. aeruginosa* AR strains were obtained from the Centers for Disease Control and Prevention and FDA Antibiotic Resistance Isolate Bank. *P. aeruginosa* Cubist strains were obtained from Cubist Pharmaceuticals in 2008. *P. aeruginosa* PA14 and PA14 Δ40 were a generous gift from D. Bumann, B. Claudi and co-workers<sup>35</sup>. *P. aeruginosa* PAO1 Δ6 was a generous gift from H. Zgurskaya and co-workers<sup>36</sup>. *P. aeruginosa* 1113 and 1727 were a generous gift from C. Llanes<sup>48</sup>. *P. aeruginosa* Carle strains were obtained from Carle Hospital in Urbana, IL, USA.

### Antimicrobial susceptibility tests

Susceptibility testing was performed in biological triplicate, using the microdilution broth method as outlined by the Clinical and Laboratory Standards Institute. Bacteria were cultured with cation-adjusted Mueller–Hinton (CAMH) broth (Sigma-Aldrich; catalogue no. 90922) or Luria–Bertani (LB) broth (Lennox) in round-bottom 96-well plates (Corning; catalogue no. 3788). To probe the magnesium-dependence of antibacterial activity, CAMH was supplemented with 5 mM MgCl<sub>2</sub>.

### Accumulation assay

The accumulation assay was performed in triplicate in batches of ten samples, with each batch containing tetracycline or ciprofloxacin as a positive control. *P. aeruginosa* PAO1, PAO1 Δ6, PA14, PA14 Δ40 and PA1280 and *E. coli* MG1655 were used in these experiments. For each replicate, 2.5 ml (*E. coli*) or 5 ml (*P. aeruginosa*) of an overnight culture were diluted into 250 ml of fresh Luria–Bertani broth (Lennox) or Tryptic Soy Broth (TSB) and grown at 37 °C with shaking to an optical density (OD<sub>600</sub>) of 0.55–0.60. The bacteria were pelleted at 3,220 rcf for 10 min at 4 °C and the supernatant was discarded. The pellets were resuspended in 40 ml of phosphate buffered saline (PBS) and pelleted as before and the supernatant was discarded. The pellets were resuspended in 8.8 ml of fresh PBS and aliquoted into ten 1.5 ml Eppendorf tubes (875 µl each). The number of colony-forming units (cfu) was determined by a calibration curve. The samples were equilibrated at 37 °C with shaking for 5 min; compound was added (final concentration 50 µM) and then the samples were incubated at 37 °C with shaking for 10 min. These time points were short enough to minimize metabolic and growth changes (no changes in OD<sub>600</sub> or cfu count observed). After incubation, 800 µl of the cultures was carefully layered on 700 µl of silicone oil (9:1 AR20/Sigma High Temperature, cooled to –78 °C). Bacteria were pelleted through the oil by centrifuging at 13,000 rcf for 2 min at room temperature (with the supernatant remaining above the oil); the supernatant and oil were then removed by pipetting. To lyse the samples, each pellet was dissolved in 200 µl of water and, then, they were subjected to three (*E. coli*) or four (*P. aeruginosa*) freeze–thaw cycles of 3 min in liquid nitrogen followed by 3 min in a water bath at 65 °C. *P. aeruginosa* samples were then treated with 50 µM DNase and RNase and incubated at 37 °C for 15 min. The lysates were pelleted at 13,000 rcf for 2 min at room temperature and the supernatant was collected (180 µl). The debris was resuspended in 100 µl of methanol and pelleted as before. The supernatants were removed and combined with the previous supernatants collected. Finally, the remaining debris was removed by centrifuging at 20,000 rcf for 10 min at room temperature. Supernatants were analysed by LC–MS/MS.

Samples were analysed with the 5500 QTRAP LC/MS/MS system (AB Sciex) with a 1200 series HPLC system (Agilent Technologies) including a degasser, an autosampler and a binary pump. Liquid chromatography separation was performed on an Agilent SB-Aq column (4.6 × 50 mm<sup>2</sup>, 5 µm) (Agilent Technologies) with mobile phase A (0.1% formic acid

in water) and mobile phase B (0.1% formic acid in acetonitrile). The flow rate was 0.3 ml min<sup>−1</sup>. The linear gradient was as follows: 0–3 min, 100% mobile phase A; 10–15 min, 2% mobile phase A; 15.5–21 min, 100% mobile phase A. The autosampler was set at 5 °C. The injection volume was 15 µl. Mass spectra were acquired with both positive electrospray ionization at the ion spray voltage of 5,500 V and negative electrospray ionization at the ion spray voltage of –4,500 V. The source temperature was 450 °C. The curtain gas, ion source gas 1 and ion source gas 2 were 33, 50 and 65, respectively. Reaction monitoring was used to quantify the metabolites. Power analysis was not used to determine the number of replicates. Error bars represent the standard error of the mean of three biological replicates. The statistical significance of the accumulation was determined using a two-sample Welch's *t*-test (one-tailed test, assuming unequal variance) relative to the negative controls. All compounds evaluated in the biological assays were at least 95% pure.

### PMBN assays

Assays measuring permeabilization by PMBN were performed as above, with the addition of 8 µg ml<sup>−1</sup> of PMBN immediately before the compound of interest was added.

### Accumulation assay with magnesium

Assays measuring the effect of magnesium treatment were performed as above, with the addition of 1 mM MgCl<sub>2</sub> immediately before the compound of interest was added.

### NPN outer-membrane permeabilization assay

An overnight culture of *P. aeruginosa* PAO1 was diluted into 10 ml of fresh TSB and grown to mid-log phase. Cells were collected by centrifugation at 3,220g for 10 min at room temperature. The supernatant was discarded and the pellet was resuspended in 5 mM HEPES (pH 7.2), 5 mM glucose. Cells were collected again by centrifugation, supernatant discarded and pellet resuspended to an OD<sub>600</sub> = 1. Then, 100 µl of washed cells and 100 µl of assay buffer containing 20 µM NPN were mixed together and added to a 96-well optical-bottom black plate. Either 2 µl of FA, FA prodrug, gentamicin, colistin or DMSO was added to each well at final concentrations of 4, 8, 16 or 32 µg ml<sup>−1</sup> and fluorescence was immediately monitored at an excitation wavelength of 350 nm and emission wavelength of 420 nm for 10 min at 30 s intervals. Fluorescence values were normalized to the control wells.

### Membrane depolarization assay

A total of 100 µl of an overnight culture of *P. aeruginosa* PAO1 was diluted into 10 ml of fresh TSB and grown to mid-log phase. Cells were collected by centrifugation at 3,220g for 10 min at room temperature. The supernatant was discarded and the pellet was resuspended in 5 mM HEPES (pH 7.8). Cells were collected again by centrifugation and supernatant discarded. The pellet was then resuspended in 5 mM HEPES with 100 mM KCl and diluted to an OD<sub>600</sub> of 0.1. A total of 0.2 M EDTA was added to the bacterial solution to a final concentration of 0.2 mM EDTA to permeabilize the bacteria to the dye. Into a black 96-well plate, 192 µl of the bacterial/EDTA solution and 8 µl of 10 µM DiSC dye were added to the wells. The fluorescence of the plate was monitored for 30 min, with reads every 5 min at the excitation wavelength of 622 nm and emission wavelength of 670 nm. To re-establish the proton gradient, 2 µl of 10 M KCl solution (final concentration of 100 mM KCl) was added to each well. 2 µl of compound was added at each concentration and fluorescence monitored for 60 min. Triton X (1%) was used as the positive control and DMSO was the negative control.

### Selection of resistant mutants

Resistant mutants were selected using the large inoculum method. Briefly, *P. aeruginosa* Δ6 (1.8 × 10<sup>9</sup> cfu) was plated on 100 mm plates of

Luria–Bertani agar containing 64, 32 or 16 µg ml<sup>-1</sup> of FA with 10 µg ml<sup>-1</sup> of gentamicin. Colonies were visible after incubating at 37 °C for 72 h. Resistant colonies were confirmed by streaking on selective media with the same concentration of FA.

### Confocal fluorescence microscopy and sample preparation

Accumulation was performed as described above for either *P. aeruginosa* PAO1 or *E. coli* MG1655 with either BIM X ( $\pm$ MgCl<sub>2</sub>) or DSMO up until the point immediately after removing the oil and supernatant and before the freeze–thaw lysis. The pellet was then resuspended in 1 ml of 3.7% formaldehyde in PBS, transferred to a new tube and allowed to sit on a nutator for 30 min at room temperature. 3 µl of the now fixed bacterial cells was placed on a clean microscope cover slip (22 × 40 mm<sup>2</sup>, VWR), followed by an agarose pad prepared as described previously<sup>49</sup>, followed by a second cover slip. Fluorescence images were taken with a Zeiss 710 multiphoton confocal microscope through a  $\times$ 63/1.4 refractive index oil objective. All samples were excited at 488 nm with an argon laser and fluorescence emission was recorded from 599 to 689 nm. Images were acquired and processed using Zen Black (Zen 2.3).

### Hydrolysis of FA prodrug

The hydrolysis of FA prodrug (10 µg ml<sup>-1</sup>) in PBS at 37 °C (shaking incubation) was monitored using LC–MS over 48 h.

### Microsomal stability

To a 1.7 ml Eppendorf tube was added PBS (442.5 µl), 20× NADPH regenerating solution A (Corning Gentest) (25 µl) and 100× NADPH regenerating solution B (Corning Gentest) (5 µl). This was placed in a shaking incubator (250 r.p.m.) for 5 min at 37 °C. To the solution was then added the compound of interest (2.5 µl of a 10 mM stock) and finally the mouse liver microsomes (Gibco Mouse (CD-1)) (25 µl, 20 mg ml<sup>-1</sup>). The solution was then mixed by pipetting and a 50 µl aliquot was removed and added to 50 µl of cold acetonitrile. This was taken to be *T* = 0 h. The remaining solution was placed back into the incubator and allowed to stand for a further 2 h before repeating this same process. Quenched samples were centrifuged at 13,000 rcf for 3 min and 75 µl of the supernatant was taken and submitted for LC–MS/MS analysis.

### Plasma stability

To a 1.7 ml Eppendorf tube was added PBS (39 µl) followed by bovine plasma (160 µl) for each assay. This was placed in a shaking incubator (250 r.p.m.) for 5 min at 37 °C. To the warm sample was then added the compound of interest (1 µl of a 10 mM stock). The samples were vortexed and a 50 µl aliquot was removed and added to 200 µl of cold acetonitrile. This was taken to be *T* = 0 h. The remaining assay was placed back into the incubator and allowed to stand for an further 2 h before repeating this process. Quenched samples were centrifuged at 16,000 rcf for 5 min and 100 µl of the supernatant was taken and submitted for LC–MS/MS analysis.

### Cytotoxicity

IC<sub>50</sub> values for FA and FA prodrug were recorded in HFF-1 cells (male, newborn; obtained from the American Type Culture Collection). Cells were seeded in a 96-well plate at 3,000 cells per well and allowed to grow for 24 h. Cells were then treated with compound and allowed to incubate for another 72 h before assessing cell viability with Alamar blue assay. The cells were not tested for mycoplasma beforehand.

### Calculation of physiochemical properties

Datasets of chemical structures were created and managed using Canvas (Schrödinger, LLC). Initial structure preparation and three-dimensional (3D) minimization was performed with LigPrep (Schrödinger) using OPLS\_2005 force fields. Generation of ensembles of conformations

was performed using Conformational Search in MOE 2015.10 using the LowModeMD method with default. Physiochemical descriptors (both 2D- and 3D-based) were calculated using MOE 2015.1049 for each conformation. Descriptors were averaged (unweighted mean) across all conformations for each molecule. Data with descriptors were used to train a random forest classification prediction model using the R package caret. The random forest model offers many advantages for this application including resistance to overfitting and the ability to measure descriptor importance<sup>50</sup>. Preprocessing of data removed descriptors with near-zero variance or high cocorrelation with other descriptors. Source code for data analysis and model training can be found at <https://github.com/HergenrotherLab/GramNegAccum>. ClogD<sub>7.4</sub> values were calculated using the online compound property calculation software FAFdrugs.

### Statistical analyses

GraphPad Prism v.8.2.1.441 was used for data analysis and figure generation. Data are shown as means  $\pm$  s.e.m. Binary accumulator or non-accumulator classification was determined by using a two sample Welch's *t*-test (one-tailed test, assuming unequal variance) relative to the negative controls. Variance in accumulation across molecules was found to be unequal by Bartlett's test. For all other experiments, statistical significance was determined using an unpaired Student's *t*-test assuming equal variance as determined by an F-test. *P* < 0.05 was considered statistically significant. In this study, no statistical methods were used to predetermine the sample size. The experiments were not randomized and the investigators were not blinded to allocation during the experiments and outcome assessments.

### Reporting summary

Further information on research design is available in the Nature Portfolio Reporting Summary linked to this article.

### Data availability

All data supporting the findings of this study are available in the paper and the Supplementary Information. Source data are provided with this paper.

### Code availability

Source code for data analysis and model training can be found at <https://github.com/HergenrotherLab/GramNegAccum>.

48. Llanes, C. et al. Clinical strains of *Pseudomonas aeruginosa* overproducing MexAB-OprM and MexXY efflux pumps simultaneously. *Antimicrob. Agents Chemother.* **48**, 1797–1802 (2004).
49. Skinner, S. O., Sepulveda, L. A., Xu, H. & Golding, I. Measuring mRNA copy number in individual *Escherichia coli* cells using single-molecule fluorescent in situ hybridization. *Nat. Protoc.* **8**, 1100–1113 (2013).
50. Breiman, L. Random forests. *Mach. Learn.* **45**, 5–32 (2001).

**Acknowledgements** We thank the NIH (AI136773), the University of Illinois and Roche for support of this work. M.K.G. is a member of the NIH Chemistry-Biology Interface Training Grant (T32-GM136629). We thank L. Li (Metabolomics Center, Roy J. Carver Biotechnology Center, UIUC and Duke University School of Medicine Proteomics and Metabolomics Core Facility) for all LC–MS/MS analysis. We thank D. Olson, L. Zhu and N. Duay at the School of Chemical Sciences NMR Laboratory at UIUC for NMR services. We thank A. Cyphersmith and the Core Facilities at the Carl Woese Institute for Genomic Biology for assistance with confocal imaging. We are grateful to all past Hergenrother laboratory members who have contributed compounds to the complexity-to-diversity collection and to B. Drown, who wrote the code used for the random forest analysis. We thank H. Zgurskaya for the generous donation of the *P. aeruginosa* PA01 Δ6 and PA01 Δ6-pore strains and D. Bumann for the generous donation of the *P. aeruginosa* PA14 and PA14 Δ40 strain. We are further grateful to collaborators at Roche, including C. Kramer who helped establish this collaboration early on and G. M. Daniel for his guidance of the collaboration as alliance manager.

**Author contributions** P.J.H. and E.J.G. conceived the study. E.J.G. performed accumulation analyses, computational analyses and mode of uptake studies with assistance of M.K.G.

# Article

E.J.G., M.R.L., M.K.G. and S.J.P. synthesized compounds in the test set. M.G.C., A.G. and M.K.G. synthesized FA derivatives. E.J.G., A.G., M.G.C. and M.K.G. performed MICs. C.B. and L.G. provided compounds and assisted with analysis of the data. E.J.G. and P.J.H. wrote this manuscript and it was approved by all authors. P.J.H. supervised this research.

**Competing interests** The University of Illinois has filed patents on some of the compounds described herein on which P.J.H. and M.G.C. are inventors.

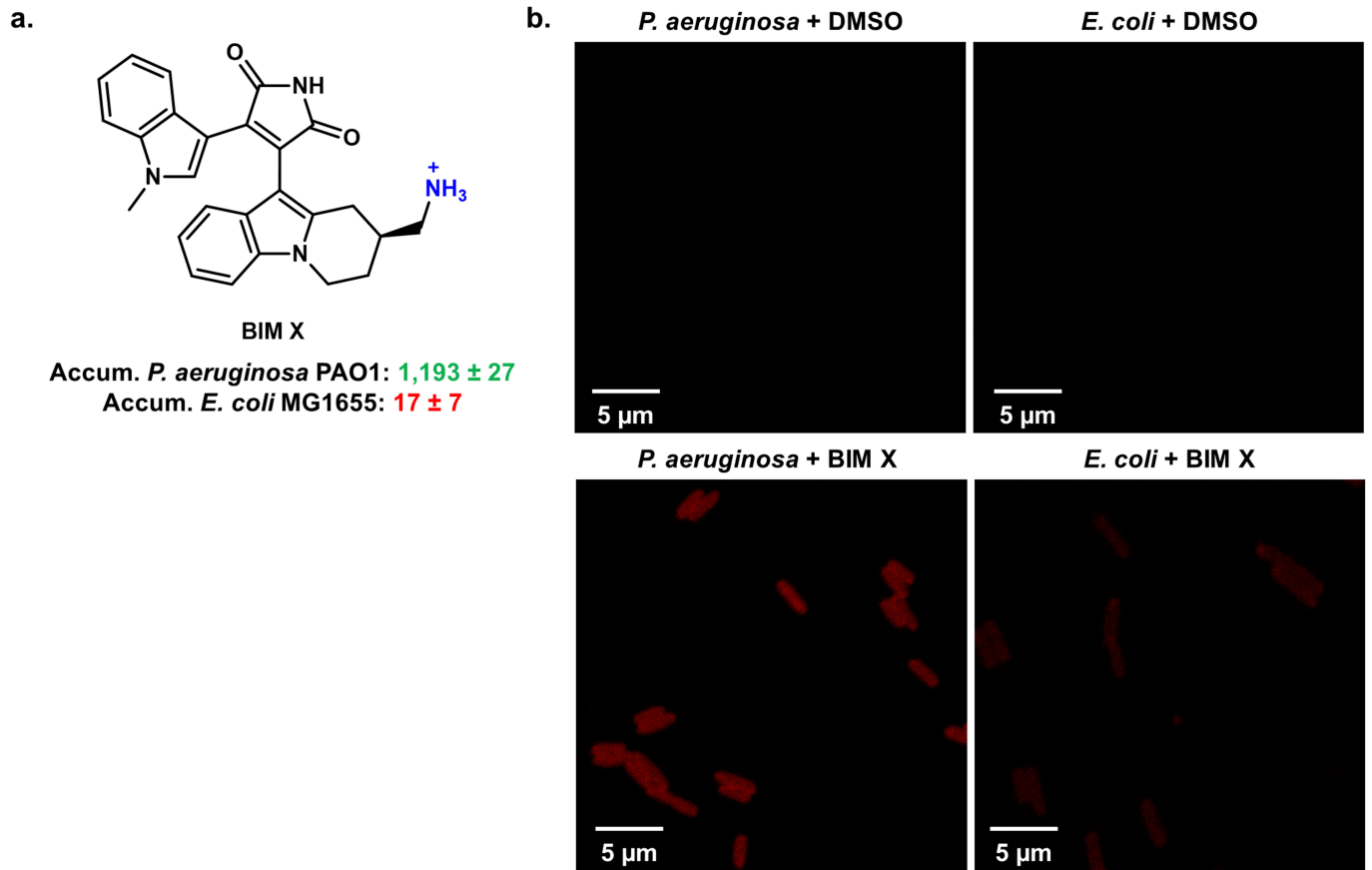
## Additional information

**Supplementary information** The online version contains supplementary material available at <https://doi.org/10.1038/s41586-023-06760-8>.

**Correspondence and requests for materials** should be addressed to Paul J. Hergenrother.

**Peer review information** *Nature* thanks Kim Lewis and the other, anonymous, reviewer(s) for their contribution to the peer review of this work.

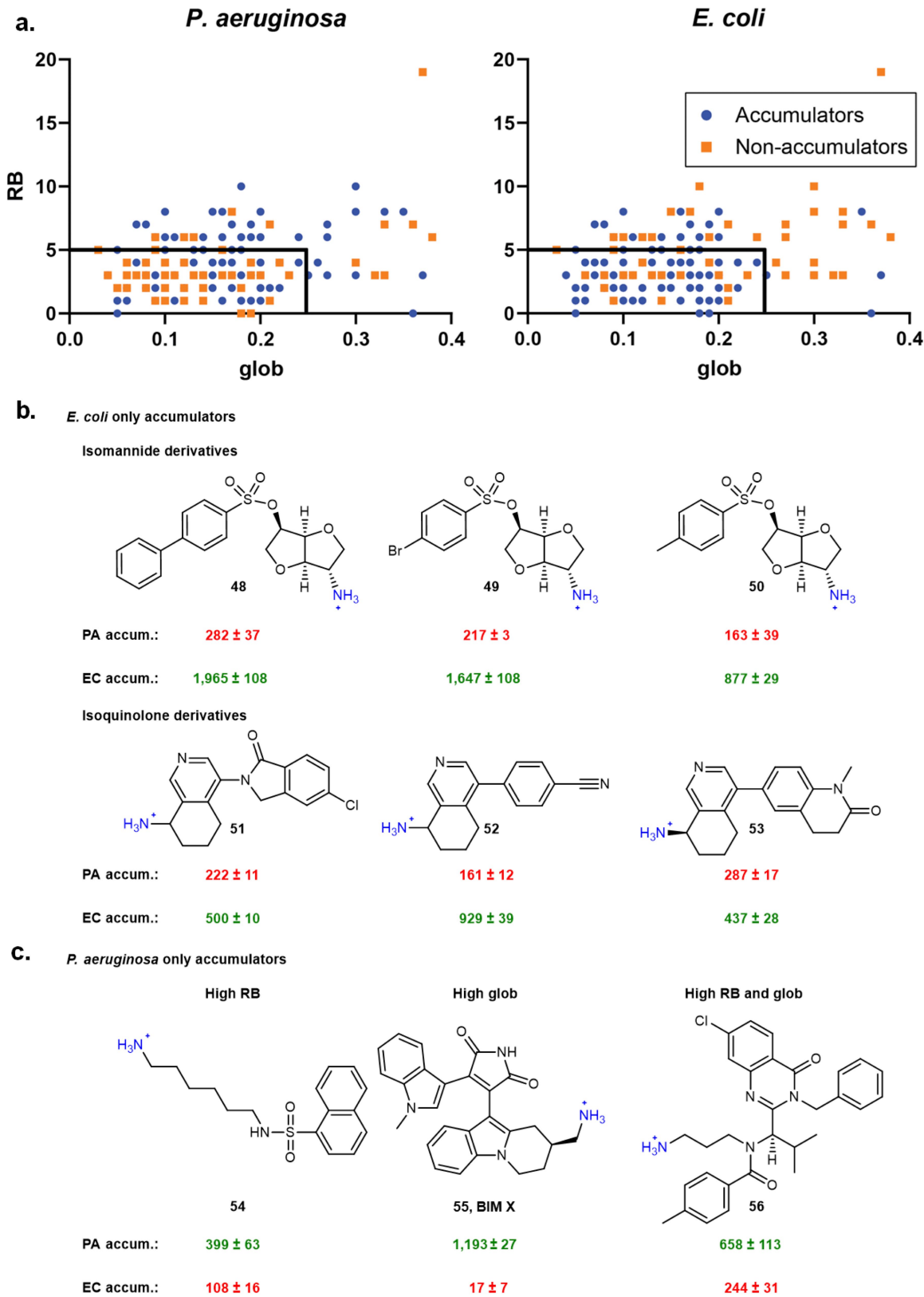
**Reprints and permissions information** is available at <http://www.nature.com/reprints>.



**Extended Data Fig. 1 | Confocal fluorescent images of an intrinsically fluorescent compound, Bisindolylmaleimide X (BIM X).** **a)** The structure of BIM X along with accumulation values. The LC-MS/MS assay reveals BIM X as a poor accumulator in *E. coli* MG1655, while it is a good accumulator in *P. aeruginosa* PAO1. Accumulation units are in nmol/10<sup>12</sup> CFU and the error is reported as the s.e.m. **b)** The standard accumulation assay was performed in *P. aeruginosa* (PAO1) and *E. coli* (MG1655) with either BIM X (50 μM) or DMSO

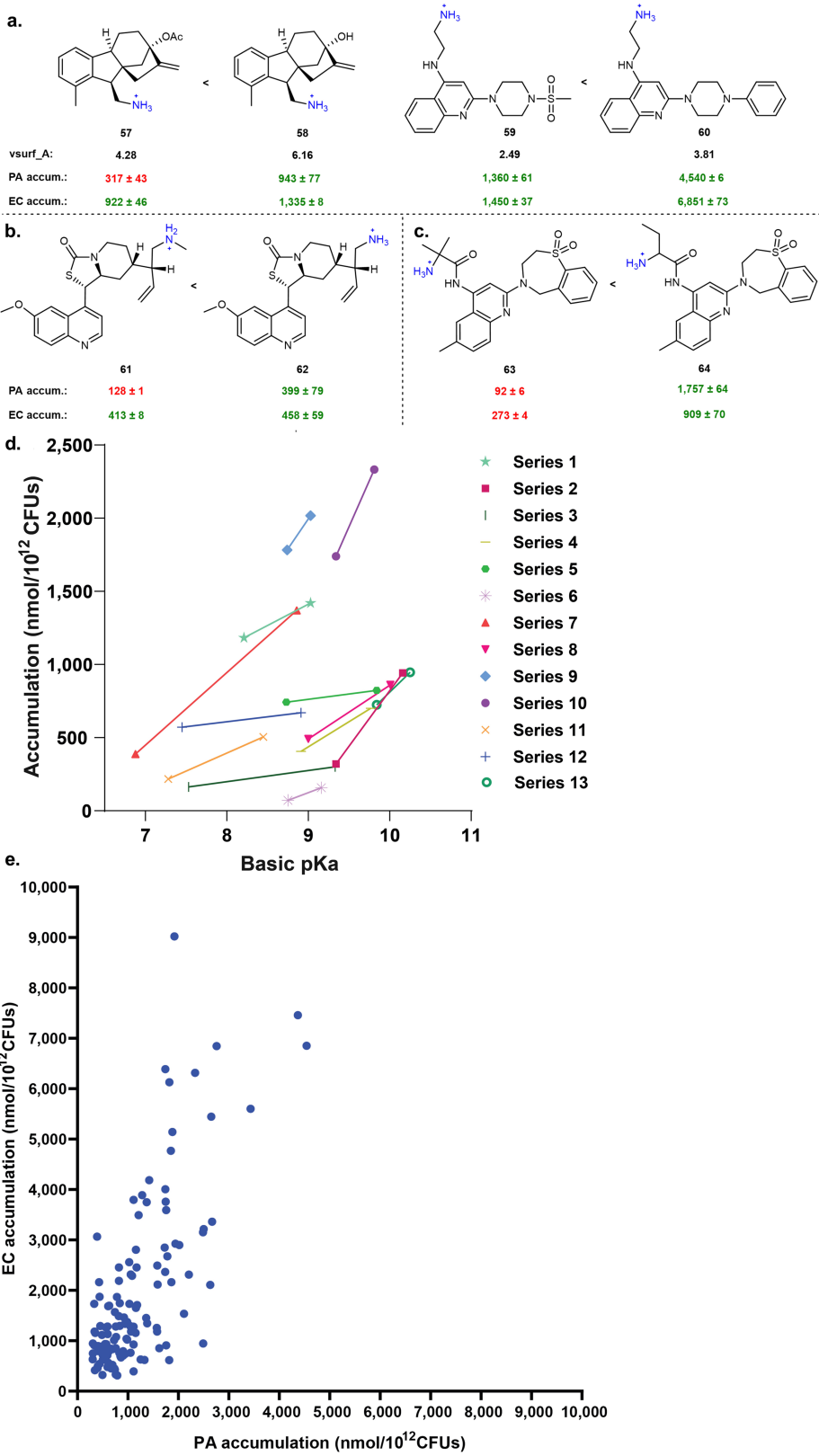
until just after the oil removal step. Cells were fixed in 3.7 % formaldehyde in PBS and fluorescence images were taken with a Zeiss 710 multiphoton confocal microscope through a 63x/1.4 oil objective. All samples were excited at 488 nm with an argon laser and fluorescence emission was recorded from 599–689 nm. Images were acquired using Zen Black (Zen 2.3). DMSO controls for both cell types tested indicate no autofluorescence. Images are representative of n = 3 biologically independent samples.

# Article



**Extended Data Fig. 2 | Comparison of species-specific accumulation trends.** **a)** In the expanded set of primary amines, many compounds that fit the eNTRy rules do not accumulate in *P. aeruginosa* PAO1 and many compounds that do not fit the eNTRy rules do accumulate in *P. aeruginosa* PAO1. Low globularity (glob) and low rotatable bonds (RB) are predictive for ~80% of compounds tested in *E. coli* MG1655, but only 41% of compounds in *P. aeruginosa* PAO1. Compounds with poor amine steric accessibility, low amphiphilic moment and multiple charges were removed from this analysis;

154 compounds total are included in the plots, see Compound Master Table for compounds. **b)** Compounds that accumulate in *E. coli*, but not in *P. aeruginosa*, can often be grouped according to structural class, but no additional trends were identified. **c)** Compounds that accumulate in *P. aeruginosa*, but not *E. coli*, are primarily compounds that have high rotatable bonds, high globularity, or both. Accumulation units are reported in nmol/10<sup>12</sup> CFUs. n = 3 biologically independent samples. The s.e.m. is reported for accumulation values.

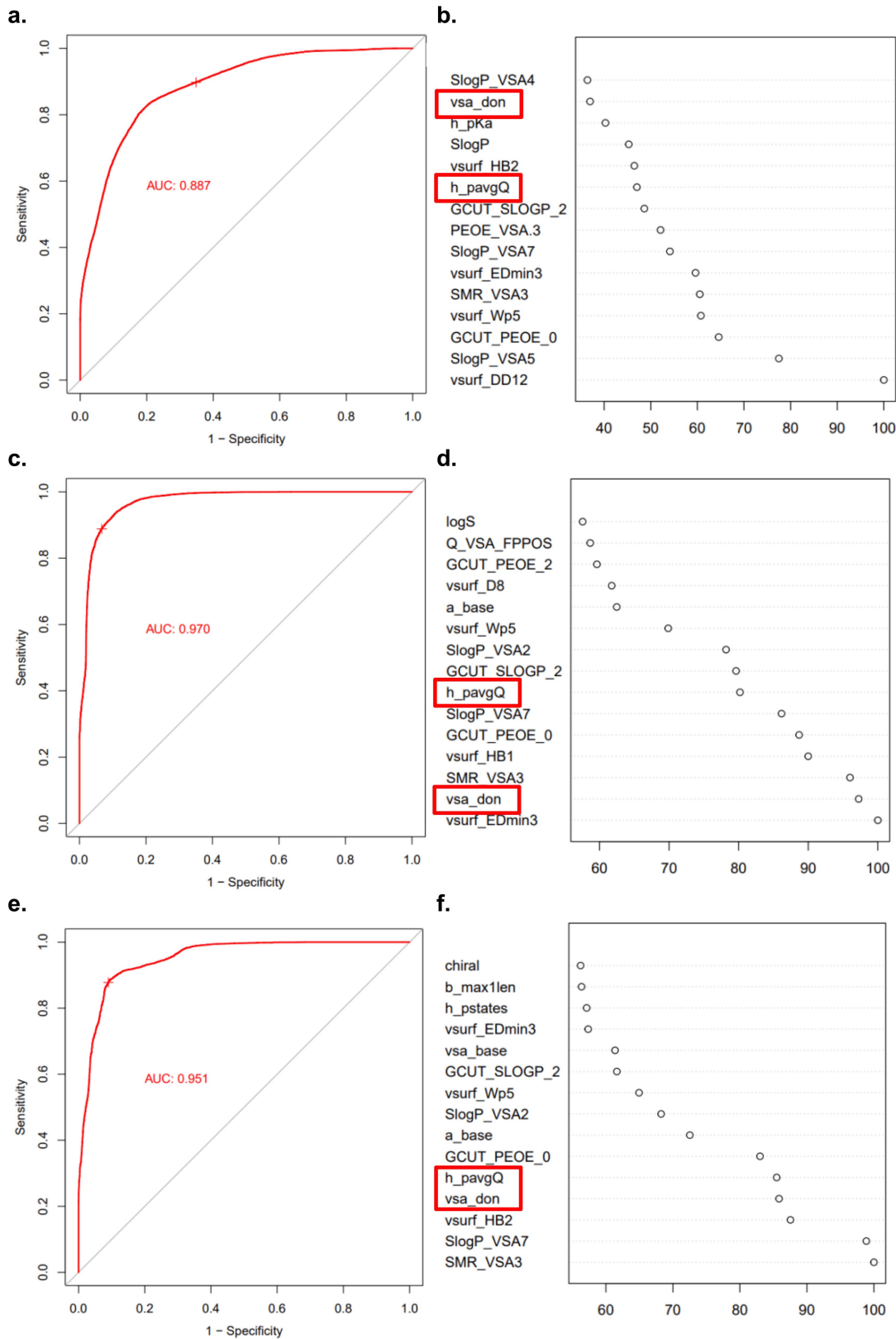


**Extended Data Fig. 3** | See next page for caption.

# Article

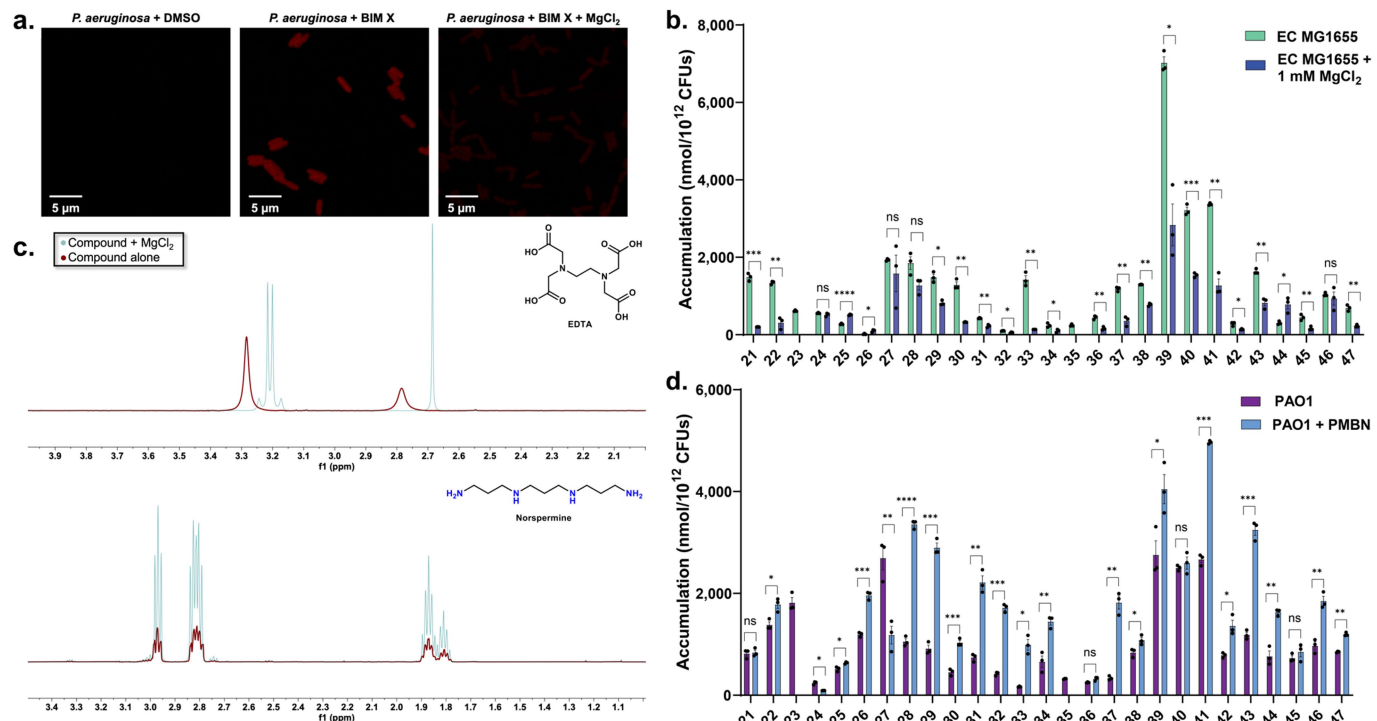
**Extended Data Fig. 3 | Accumulation trends, matched molecular pairs and comparison of *P. aeruginosa* and *E. coli* accumulation.** **a)** Amphiphilic moment (vsurf\_A) positively correlates with accumulation in both *P. aeruginosa* and *E. coli*. **b)** Amine steric accessibility is important for accumulation in both *P. aeruginosa* and *E. coli*. **c)** Similarly, compounds with primary amines on secondary carbons tend to accumulate higher than compounds with primary amines on tertiary carbons. **d)** Matched molecular pairs show a correlation between amine pK<sub>a</sub> and accumulation in *P. aeruginosa*. For structures, see

Supplementary Table 8. The pK<sub>a</sub> estimation was calculated using the software MoKa (v3.2.2) from Molecular Discovery suite. **e)** Distribution of accumulation values in *P. aeruginosa* vs. *E. coli* for compounds that accumulate in both bacterial strains (131 compounds plotted, see Compound Master Table for structures). Accumulation levels were lower on average in *P. aeruginosa* PAO1 relative to *E. coli* MG1655. Accumulation units are reported in nmol/10<sup>12</sup> CFUs. n = 3 biologically independent samples. The s.e.m. is reported for accumulation values. Strains used: *E. coli* MG1655, *P. aeruginosa* PAO1.



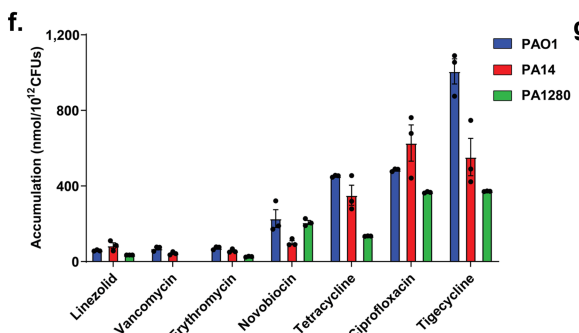
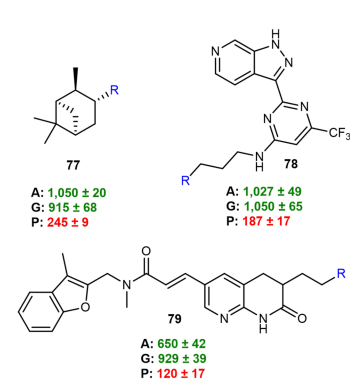
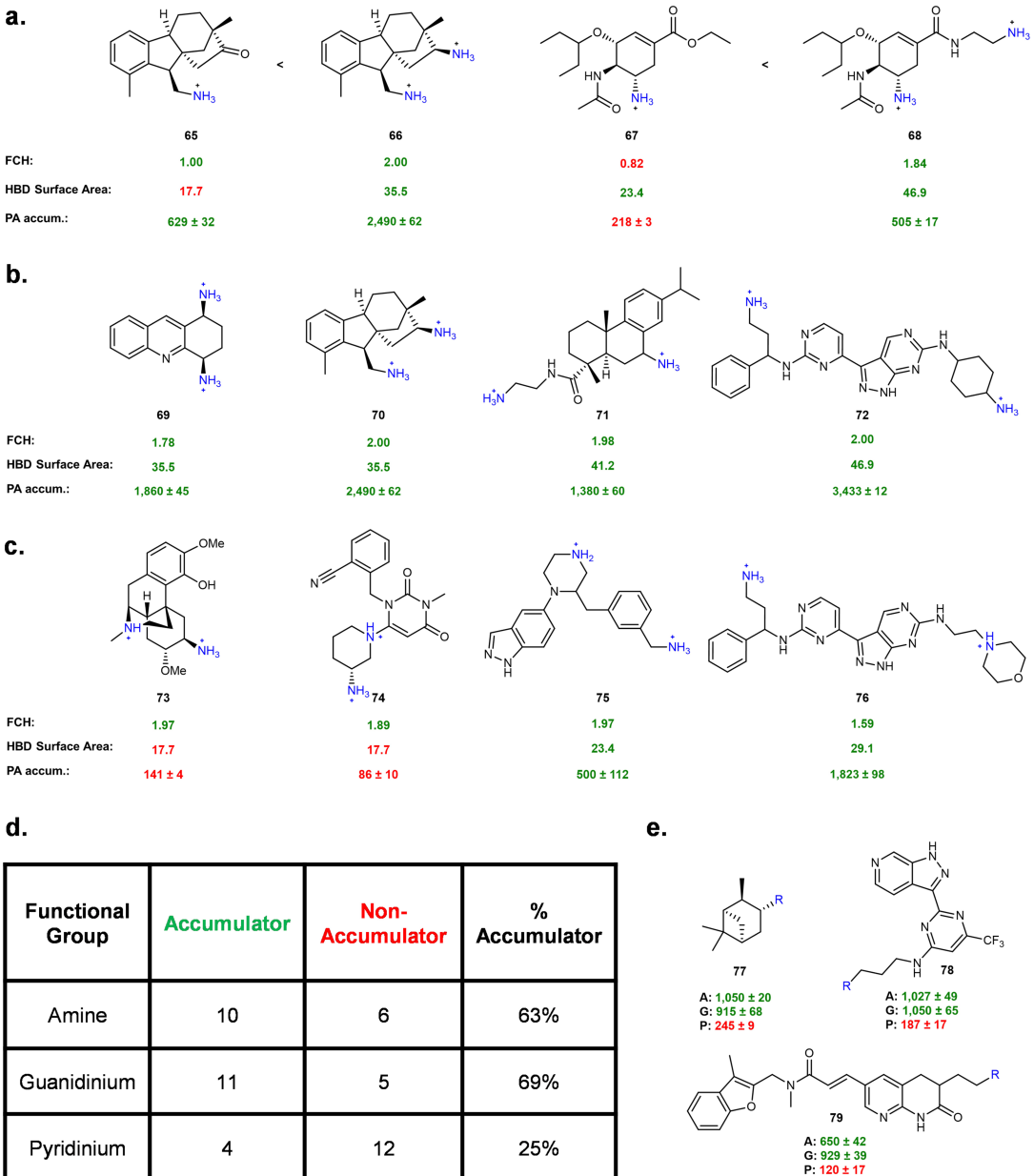
**Extended Data Fig. 4 | Random forest prediction modelling.** **a)** Random forest prediction model results on dataset of all 240 primary amines, structures reported in Supplementary Table 2. ROC plot with 10 repeated cross-validations in the training classification models. **b)** Relative importance of top 15 descriptors for all 240 primary amines. **c)** Random forest prediction model results on dataset of 50 highest primary amine accumulators and 50 lowest primary amine accumulators (100 amines total; compounds **2.1-2.50; 2.191-2.240** in Supplementary Table 2). **d)** Relative importance of top 15 descriptors for 100 primary amines. **e)** Random forest prediction model results on dataset of 30 highest primary amine accumulators and 30 lowest primary amine accumulators (60 amines total; compounds **2.1-2.30; 2.211-2.240** in Supplementary Table 2). **f)** Relative importance of top 15 descriptors for 60 primary amines. Formal charge (*h\_pavgQ*) and hydrogen bond donor surface area (*vsa\_don*) are boxed in red. Early iterations of the model with the incomplete compound library always identified these properties within the top 15 most important.

descriptors for 100 primary amines. **e)** Random forest prediction model results on dataset of 30 highest primary amine accumulators and 30 lowest primary amine accumulators (60 amines total; compounds **2.1-2.30; 2.211-2.240** in Supplementary Table 2). **f)** Relative importance of top 15 descriptors for 60 primary amines. Formal charge (*h\_pavgQ*) and hydrogen bond donor surface area (*vsa\_don*) are boxed in red. Early iterations of the model with the incomplete compound library always identified these properties within the top 15 most important.



**Extended Data Fig. 5 | Influence of magnesium on accumulation, evaluation of its binding by NMR and influence of magnesium and PMBN on compound accumulation.** **a)** Confocal fluorescent images of an intrinsically fluorescent compound, Bisindolylmaleimide X (BIM X) in *P. aeruginosa* with or without  $MgCl_2$ . The standard accumulation assay was performed in *P. aeruginosa* (PAO1) with either DMSO, BIM X (50  $\mu M$ ), or BIM X (50  $\mu M$ ) +  $MgCl_2$  (1 mM), until just after the oil removal step. Cells were fixed in 3.7% formaldehyde in PBS and fluorescence images were taken with a Zeiss 710 multiphoton confocal microscope through a 63x/1.4 oil objective. All samples were excited at 488 nm with an argon laser and fluorescence emission was recorded from 599–689 nm. Images were acquired using Zen Black (Zen 2.3). The images for *P. aeruginosa* + DMSO and *P. aeruginosa* + BIM X are the same as in Extended Data Fig. 1. DMSO controls indicate no autofluorescence. Images are representative of  $n = 3$  biologically independent samples. **b)** Evaluation of accumulation of compounds in *E. coli* MG1655 upon cotreatment with  $MgCl_2$  (1 mM). **c)** Determination of  $Mg^{2+}$  interactions with polyamines. Ethylenediaminetetraacetic acid (EDTA), a compound known to chelate to  $Mg^{2+}$  in solution, clearly shows a marked chemical shift change in the NMR as well as changes in coupling when comparing EDTA alone to EDTA plus  $Mg^{2+}$ . When this same experiment was performed with

norspermine, there were no observable changes in coupling or chemical shift in the presence of  $MgCl_2$ , suggesting a lack of perturbation of any electronic environment on the molecule, thus, a lack of interaction between  $Mg^{2+}$  and norspermine. Compounds were evaluated at a final concentration of 1 mM and  $MgCl_2$  was at a final concentration of 20 mM to maintain the same  $Mg^{2+}$ -to-compound ratio as in the accumulation experiments. The pD of all solutions was adjusted to 7.2 prior to analysis. **d)** The same set of compounds as in Extended Data Fig. 5b showed a statistically significant increase in accumulation in *P. aeruginosa* PAO1 upon cotreatment with the permeabilizer PMBN (8  $\mu g/ml$ ). All structures and accumulation values are listed in Supplementary Table 4b. For samples with additives in Extended Data Fig. 5b & d, compounds 23 and 35 did not meet the mass spec standards and are thus excluded from this analysis.  $n = 3$  biologically independent samples. The average and s.e.m are reported for accumulation values. Statistical significance was determined using a two-sample Welch's *t*-test (one-tailed test, assuming unequal variance). Statistically significant accumulation differences for compounds in *P. aeruginosa* PA14 versus *P. aeruginosa* PA14 with PMBN treatment or *E. coli* MG1655 versus *E. coli* MG1655 with  $MgCl_2$  treatment are indicated with asterisks (n.s. not significant, \* $P < 0.05$ , \*\* $P < 0.01$ , \*\*\* $P < 0.001$ , \*\*\*\* $P < 0.0001$ ).



**g.**

Strain	Accumulator	Non-Accumulator	% concordance with PAO1
PAO1	14	13	100%
PA14	16	11	93%
PA1280	13	14	96%

Extended Data Fig. 6 | See next page for caption.

# Article

**Extended Data Fig. 6 | Multiple amines and alternative positive charges often aid in accumulation in *P. aeruginosa* PAO1.** **a)** Diamines accumulate to significantly higher levels intracellularly in *P. aeruginosa* relative to their monoamine comparators. **b)** Diamines containing two primary amines consistently accumulate to a significant extent. **c)** Diamines containing one primary amine and one secondary or tertiary amine have more variable accumulation levels in *P. aeruginosa*, depending on hydrogen bond donor ability. **d)** Accumulation summary of 16 amine, guanidinium and pyridinium containing compounds (48 compounds total, structures in Supplementary Table 5) in *P. aeruginosa* PAO1. Compounds are classified as accumulators or non-accumulators based on statistical significance relative to the negative antibiotic controls. **e)** Examples of side-by-side amine (A), guanidinium (G) and pyridinium (P) comparators and their relative accumulation values in *P. aeruginosa* PAO1. Amine and guanidinium comparators tend to accumulate

to a very similar extent, while pyridiniums often do not accumulate to a significant extent. **f)** Accumulation of antibiotic controls in three *P. aeruginosa* strains. Accumulation is consistent with antibacterial activity reported in Extended Data Table 1c. **g)** Accumulation of representative non-antibiotics in three *P. aeruginosa* strains. While there is some variance in accumulation levels between strains, high concordance of accumulation classification was observed. Compounds are classified as accumulators or non-accumulators based on statistical significance relative to the negative antibiotic controls. Structures and accumulation values are reported in Supplementary Table 6. Accumulation units are reported in nmol/10<sup>12</sup> CFUs. n = 3 biologically independent samples. The average and s.e.m. are reported for accumulation values. Accumulation units are reported in nmol/10<sup>12</sup> CFUs. All compounds were tested in biological triplicate. The average and s.e.m. are reported for accumulation values. Formal charge (FCH) was calculated using MOE.

a.	MIC values ( $\mu\text{g/mL}$ )		Accumulation	
	<i>E. coli</i> MG1655	<i>P. aeruginosa</i> PAO1	<i>E. coli</i> MG1655	<i>P. aeruginosa</i> PAO1
FA	512	1,024	52 $\pm$ 5	169 $\pm$ 14
FA prodrug 2	256	>256*	969 $\pm$ 41	1,011 $\pm$ 29
FA prodrug 3	32	128	1,764 $\pm$ 21	1,247 $\pm$ 58
FA prodrug	4	8	3,337 $\pm$ 101	2,240 $\pm$ 78

MIC fold change of FA prodrug in growth media	EF-G mutation	MIC of FA prodrug ( $\mu\text{g/mL}$ )	Fold change in MIC vs. WT <i>E. coli</i> MG1655
2X	P414Q	16	4X
4X	P414Q	16-32	4X-8X
8X	R472L	16-32	4X-8X

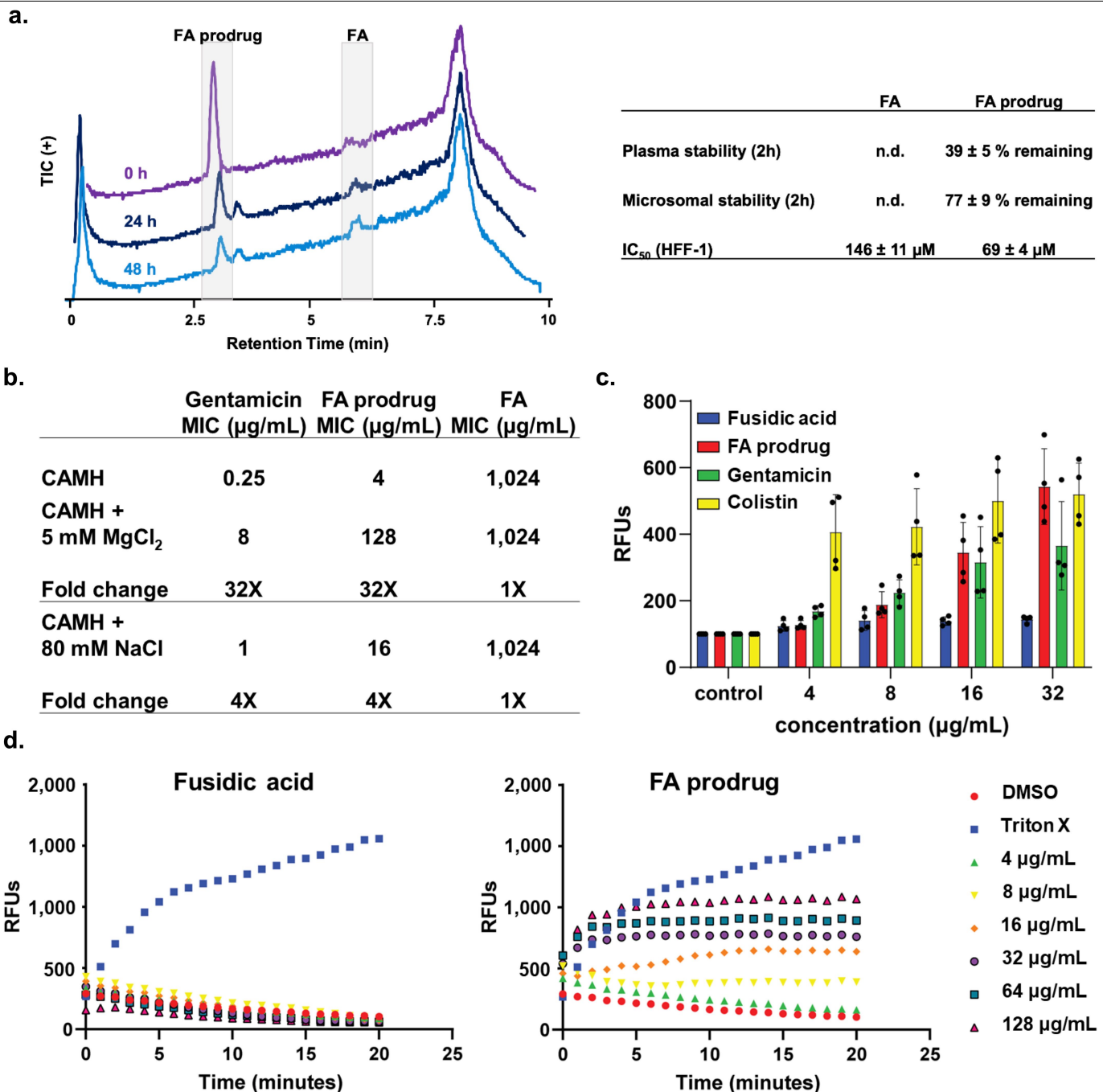
c.	FA	FA Ac <sub>2</sub> O	FA prodrug	FA prodrug Ac <sub>2</sub> O
<i>S. aureus</i> ATCC 29213	0.125	64	1	16
<i>E. coli</i> MG1655	512	>512*	4	16
<i>P. aeruginosa</i> PAO1	1,024	>512*	8	32

Extended Data Fig. 7 | See next page for caption.

# Article

**Extended Data Fig. 7 | Accumulation and activity of FA and various derivatives and resistance generation in *E. coli*.** **a)** Introducing a hydrolyzable amidoxime linker onto FA provides a strategy to increase gram-negative activity and accumulation. Increasing the number of amines on the linker results in improved antibacterial activity and accumulation in two gram-negative species, *E. coli* MG1655 and *P. aeruginosa* PAO1, with the 4-amine linker-containing FA derivative (**FA prodrug**) demonstrating the most potent activity and highest absolute accumulation values. Accumulation values are reported in nmol/10<sup>12</sup> CFUs and represent the concentration of free FA in the cell. n = 3 biologically independent samples. The average and s.e.m. are reported for accumulation values. **b)** *E. coli* MG1655 mutants resistant to **FA prodrug** were generated using a serial passage method and exhibit amino acid mutations mapping back to the FA binding pocket of EF-G. Bacteria (1×10<sup>8</sup> CFU/ml) were

first inoculated in a standard MIC experiment against both sub- and supra-MIC antibiotic concentrations. The well containing the highest concentration of **FA prodrug** where bacterial growth was still observed was then isolated and re-subjected to this experiment. **c)** Acetylation of both alcohols of FA greatly disrupts target engagement of FA with EF-G as inferred from MIC values against *S. aureus*. The diacetylated version of **FA prodrug** (**FA prodrug Ac<sub>2</sub>O**) loses 4–16x activity against both gram-positive and gram-negative bacterial strains, suggesting that inhibition of EF-G contributes to the observed antibacterial activity of **FA prodrug**. MICs were performed in MH or LB broth per Clinical and Laboratory Standards Institute (CLSI) guidelines. Accumulation values are reported in nmol/10<sup>12</sup> CFUs and represent the concentration of free FA in the cell. n = 3 biologically independent samples. The average and s.e.m. are reported for accumulation values. \*Indicates compound solubility limit.



**Extended Data Fig. 8 | Mode of uptake and membrane interactions of FA prodrug.** **a)** (LEFT) In PBS at 37 °C, FA prodrug (10  $\mu$ g/ml) hydrolyses to FA (FA) over a period of 48 h, as monitored via LC-MS. TIC LC-MS traces showing the disappearance of FA prodrug and the appearance of FA. Traces are all normalized to 2E6 ion counts. (RIGHT) Plasma stability, microsomal stability and 72-hour  $IC_{50}$  values for FA and FA prodrug. Average percentage errors are reported as s.e.m.  $IC_{50}$  errors reported as s.d. n = 3 biologically independent samples. **b)** Cotreatment with magnesium ions leads to a 32x increase in MIC for gentamicin and FA prodrug, while FA shows no change. Treatment with 80 mM NaCl shows minimal change when compared to the MgCl<sub>2</sub> treated samples. MICs performed in *P. aeruginosa* PAO1 according to CLSI guidelines and values

are reported in  $\mu$ g/ml. n = 3 biologically independent samples. **c)** FA prodrug, gentamicin and colistin all permeabilize the outer-membrane of *P. aeruginosa* PAO1 to the membrane impermeable fluorophore NPN at a 10-minute time point, while treatment with FA shows no effect. Error bars represent the standard deviation from the average of RFUs. n = 3 biologically independent samples. **d)** Treatment with FA prodrug leads to dose-dependent inner-membrane depolarization in *P. aeruginosa* PAO1, quantified using the potentiometric dye DiSC<sub>3</sub>(5), while treatment with FA shows no effect. Concentrations of FA and FA prodrug are listed in  $\mu$ g/ml. 1% Triton X was used as the positive control, while 2% DMSO was used as the negative control. n = 3 biologically independent samples.

# Article

**Extended Data Table 1 | MIC values of antibiotics against *P. aeruginosa***

a.

Compound	PAO1 MIC ( $\mu\text{g/mL}$ )	PAO1 + PMBN MIC ( $\mu\text{g/mL}$ )
<b>Inactive antibiotics</b>		
Linezolid	>512	n.d.
Vancomycin	>512	n.d.
Erythromycin	256	n.d.
Fusidic acid	>512	4
Valnemulin	256	1
Novobiocin	>512	1
<b>Active antibiotics</b>		
Tetracycline	16	n.d.
Ciprofloxacin	0.5	n.d.
Tigecycline	1	n.d.

b.

Compound	PAO1 MIC ( $\mu\text{g/mL}$ )	PAΔ6 MIC ( $\mu\text{g/mL}$ )	Fold change
<b>Poor Efflux Substrate</b>			
Vancomycin	>512	>512	1
<b>Good Efflux Substrates</b>			
Chloramphenicol	>512	4	>128
Valnemulin	256	0.125	2048
Trimethoprim	>512	2	>256
Nalidixic acid	>128	2	>64
Tedizolid	>256	16	>16

c.

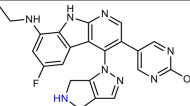
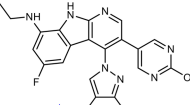
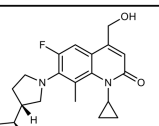
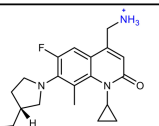
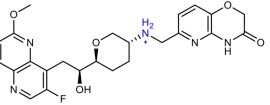
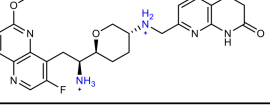
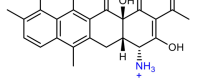
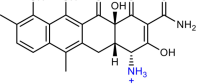
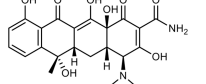
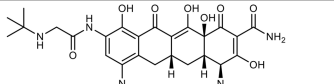
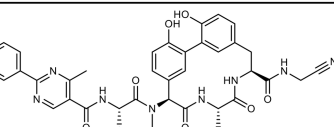
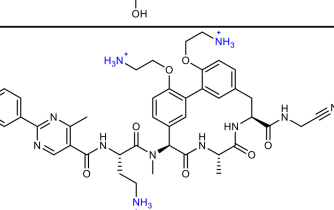
Compound	PAO1 MIC ( $\mu\text{g/mL}$ )	PA14 MIC ( $\mu\text{g/mL}$ )	PA1280 MIC ( $\mu\text{g/mL}$ )
<b>Inactive antibiotics</b>			
Linezolid	>512	>512	>512
Vancomycin	>512	>512	>512
Erythromycin	256	256	256
Novobiocin	>512	>512	>512
<b>Active antibiotics</b>			
Tetracycline	16	8	32
Ciprofloxacin	0.5	0.125	0.5
Tigecycline	1	2	16

d.

Compound	WT MIC ( $\mu\text{g/mL}$ )	PAΔ6 MIC ( $\mu\text{g/mL}$ )	Fold change	WT Accum	PAΔ6 Accum	Fold change
Chloramphenicol	>512	4	>128	114 $\pm$ 14	537 $\pm$ 11	4.7
Trimethoprim	>512	2	>256	127 $\pm$ 6	465 $\pm$ 6	3.6
Sulfamethoxazole	>64	4	>16	101 $\pm$ 26	420 $\pm$ 15	4.2
Tetracycline	16	0.25	64	452 $\pm$ 3	n.v.	-

**a)** MICs of antibiotic controls used in the accumulation assay against *P. aeruginosa* PAO1 and with cotreatment of 8  $\mu\text{g}/\text{mL}$  of PMBN. **b)** MIC ratios between *P. aeruginosa* PAO1 and *P. aeruginosa* PAΔ6 indicate whether a compound is subject to efflux. Vancomycin shows no potentiation in the efflux pump KO strain, indicating it is not liable to significant efflux, whereas chloramphenicol, valnemulin, trimethoprim, nalidixic acid and tedizolid show substantial improvements in antibacterial activity in the efflux pump KO strain, indicating these compounds have considerable efflux liabilities. **c)** MICs of antibiotic controls in three different strains of *P. aeruginosa*. **d)** Many broad-spectrum antibacterials have limited efficacy against *P. aeruginosa* because of poor accumulation, not because of a lack of target engagement. In an efflux pump-deficient strain of *P. aeruginosa*, PAΔ6<sup>26</sup>, antibiotics demonstrate significantly improved activity compared to the wild-type (WT) strain *P. aeruginosa* PAO1, along with increased intracellular accumulation. MICs were performed in MH or LB broth per Clinical and Laboratory Standards Institute (CLSI) guidelines. Accumulation units are reported in nmol/10<sup>10</sup> CFUs. The s.e.m. is reported for accumulation values. n.v. = not viable. MICs were performed in MH or LB broth per Clinical and Laboratory Standards Institute (CLSI) guidelines. n=3 biologically independent samples.

**Extended Data Table 2 | Biological data on compounds included in the retrospective analysis comparing the properties of PA-active compounds versus less active derivatives**

Structure	Compound ID	WT PA MIC	PA efflux KO MIC	WT EC MIC	$\Delta\text{tolC}$ EC MIC
	17x	10	n.r.	0.81	n.r.
	17r	1.3	n.r.	0.31	n.r.
	AMQ-1 (11 in original manuscript)	16	4	16	0.25*
	AMQ-2 (10 in original manuscript)	2	0.5	1	0.06*
	THP-1 (4 in original manuscript)	4	n.r.	0.5	0.004
	THP-2 (21 in original manuscript)	1	n.r.	0.063	0.008
	CHD	16	n.r.	n.r.	0.5
	CDCHD	1	n.r.	n.r.	0.25
	Tetracycline	16	0.25	1	0.25
	Tigecycline	1	0.125	0.5	0.125
	G8126	>64	n.r.	32	n.r.
	G0775	2	n.r.	0.125	0.063

MICs reported in  $\mu\text{g}/\text{mL}$ . n.r. = not reported. \* indicates that the MIC of compounds was determined in the *E. coli*  $\Delta\text{acrB}$  efflux mutant instead of the  $\Delta\text{tolC}$  efflux mutant.

Corresponding author(s): Paul J. Hergenrother

Last updated by author(s): Sep 19, 2023

## Reporting Summary

Nature Portfolio wishes to improve the reproducibility of the work that we publish. This form provides structure for consistency and transparency in reporting. For further information on Nature Portfolio policies, see our [Editorial Policies](#) and the [Editorial Policy Checklist](#).

### Statistics

For all statistical analyses, confirm that the following items are present in the figure legend, table legend, main text, or Methods section.

n/a Confirmed

- The exact sample size ( $n$ ) for each experimental group/condition, given as a discrete number and unit of measurement
- A statement on whether measurements were taken from distinct samples or whether the same sample was measured repeatedly
- The statistical test(s) used AND whether they are one- or two-sided  
*Only common tests should be described solely by name; describe more complex techniques in the Methods section.*
- A description of all covariates tested
- A description of any assumptions or corrections, such as tests of normality and adjustment for multiple comparisons
- A full description of the statistical parameters including central tendency (e.g. means) or other basic estimates (e.g. regression coefficient) AND variation (e.g. standard deviation) or associated estimates of uncertainty (e.g. confidence intervals)
- For null hypothesis testing, the test statistic (e.g.  $F$ ,  $t$ ,  $r$ ) with confidence intervals, effect sizes, degrees of freedom and  $P$  value noted  
*Give  $P$  values as exact values whenever suitable.*
- For Bayesian analysis, information on the choice of priors and Markov chain Monte Carlo settings
- For hierarchical and complex designs, identification of the appropriate level for tests and full reporting of outcomes
- Estimates of effect sizes (e.g. Cohen's  $d$ , Pearson's  $r$ ), indicating how they were calculated

*Our web collection on [statistics for biologists](#) contains articles on many of the points above.*

### Software and code

Policy information about [availability of computer code](#)

Data collection	Not applicable.
Data analysis	<p>Custom code: Source code for data analysis and model training for local use is available on Github (<a href="https://github.com/HergenrotherLab/GramNegAccum">https://github.com/HergenrotherLab/GramNegAccum</a>)</p> <p>Commercial software used for data analysis: GraphPad Prism 9.3.1. was used for data analysis for compound accumulation in bacteria and membrane-activity assays. Excel was used for MIC determination. Schrodinger Suite and MOE were used for ligand optimization and physicochemical property calculation. MNova was used for NMR analysis.</p>

For manuscripts utilizing custom algorithms or software that are central to the research but not yet described in published literature, software must be made available to editors and reviewers. We strongly encourage code deposition in a community repository (e.g. GitHub). See the Nature Portfolio [guidelines for submitting code & software](#) for further information.

## Data

Policy information about [availability of data](#)

All manuscripts must include a [data availability statement](#). This statement should provide the following information, where applicable:

- Accession codes, unique identifiers, or web links for publicly available datasets
- A description of any restrictions on data availability
- For clinical datasets or third party data, please ensure that the statement adheres to our [policy](#)

All data is available in the main text or the supplementary information.

## Human research participants

Policy information about [studies involving human research participants and Sex and Gender in Research](#).

### Reporting on sex and gender

*Use the terms sex (biological attribute) and gender (shaped by social and cultural circumstances) carefully in order to avoid confusing both terms. Indicate if findings apply to only one sex or gender; describe whether sex and gender were considered in study design whether sex and/or gender was determined based on self-reporting or assigned and methods used. Provide in the source data disaggregated sex and gender data where this information has been collected, and consent has been obtained for sharing of individual-level data; provide overall numbers in this Reporting Summary. Please state if this information has not been collected. Report sex- and gender-based analyses where performed, justify reasons for lack of sex- and gender-based analysis.*

### Population characteristics

*Describe the covariate-relevant population characteristics of the human research participants (e.g. age, genotypic information, past and current diagnosis and treatment categories). If you filled out the behavioural & social sciences study design questions and have nothing to add here, write "See above."*

### Recruitment

*Describe how participants were recruited. Outline any potential self-selection bias or other biases that may be present and how these are likely to impact results.*

### Ethics oversight

*Identify the organization(s) that approved the study protocol.*

Note that full information on the approval of the study protocol must also be provided in the manuscript.

## Field-specific reporting

Please select the one below that is the best fit for your research. If you are not sure, read the appropriate sections before making your selection.

Life sciences       Behavioural & social sciences       Ecological, evolutionary & environmental sciences

For a reference copy of the document with all sections, see [nature.com/documents/nr-reporting-summary-flat.pdf](https://nature.com/documents/nr-reporting-summary-flat.pdf)

## Life sciences study design

All studies must disclose on these points even when the disclosure is negative.

Sample size	No statistical methods were used to predetermine samples size.
Data exclusions	No data exclusions.
Replication	We have three or more biological replicates as indicated in the manuscript for MIC determination, compound accumulation studies, and membrane-activity assays.
Randomization	The experiments were not randomized.
Blinding	Investigators were not blinded

## Reporting for specific materials, systems and methods

We require information from authors about some types of materials, experimental systems and methods used in many studies. Here, indicate whether each material, system or method listed is relevant to your study. If you are not sure if a list item applies to your research, read the appropriate section before selecting a response.

**Materials & experimental systems**

n/a	Involved in the study
<input checked="" type="checkbox"/>	Antibodies
<input type="checkbox"/>	Eukaryotic cell lines
<input checked="" type="checkbox"/>	Palaeontology and archaeology
<input checked="" type="checkbox"/>	Animals and other organisms
<input checked="" type="checkbox"/>	Clinical data
<input checked="" type="checkbox"/>	Dual use research of concern

**Methods**

n/a	Involved in the study
<input checked="" type="checkbox"/>	ChIP-seq
<input checked="" type="checkbox"/>	Flow cytometry
<input checked="" type="checkbox"/>	MRI-based neuroimaging

**Eukaryotic cell lines**Policy information about [cell lines and Sex and Gender in Research](#)

Cell line source(s)

HFF-1 cells (male, newborn) were obtained from ATCC.

Authentication

Cell lines were authenticated by a commercial vendor and inspected visually in house.

Mycoplasma contamination

The cells were not tested for mycoplasma contamination.

Commonly misidentified lines  
(See [ICLAC](#) register)

N/A